MASTER IN BIOCHEMISTRY AND MOLECULAR AND CELLULAR BIOLOGY

Downstream analysis of Tn-seq data and characterization of ialB and oppB genes from Brucella abortus

Godessart, Pierre

Award date:
2017

Awarding institution:
University of Namur

UNIVERSITÉ DE NAMUR

Faculté des Sciences

Downstream analysis of Tn-seq data and characterization of *ialB* and *oppB* genes from *Brucella abortus*

Mémoire présenté pour l'obtention

du grade académique de master 120 en biochimie et biologie moléculaire et cellulaire

Pierre Godessart

Janvier 2017

Université de Namur
FACULTE DES SCIENCES
Secrétariat du Département de Biologie
Rue de Bruxelles, 61 - 5000 NAMUR
Téléphone: + 32(0)81.72.44.18 - Téléfax: + 32(0)81.72.44.20
E-mail: joelle.jonet@unamur.be - http://www.unamur.be

Analyse de données résultantes d'un Tn-seq et caractérisation des gènes *ialB* et *oppB* de *Brucella abortus*

GODESSART Pierre

Résumé

Faisant partie des alpha-proteobactéries, le genre *Brucella*, est composé de pathogènes intracellulaires facultatifs. Un de ses membres, *Brucella abortus,* est l'agent pathogène responsable de la brucellose bovine. Récemment, un Tn-seq a été réalisé et reposait sur une grande banque de mutants transpositionnels de *B. abortus.* Le but était de mettre en évidence des gènes requis pour le bon déroulement de l'infection de macrophages. Basé sur ces résultats, ce travail s'est focalisé sur deux gènes reportés comme importants à 2 h post infection. Le premier (BAB1_0491) est homologue à *ialB*, tandis que le second (BAB2_0701) fait partie d'un ABC transporteur à oligopeptides, homologue à Opp. Alors que IalB a été identifiée comme un facteur nécessaire au parasitisme d'érythrocytes humains par *Bartonella bacilliformis*, Opp semble posséder de nombreuses fonctions. Le but de ce mémoire était de caractériser leurs différentes fonctions chez *B. abortus*.
Dans un premier temps, des mutants de disruption *ialB* ou *oppB* ont été construits afin de procéder à des infections de macrophages. Durant ces infections, le mutant *ialB* a montré une survie amoindrie. Si le mutant *oppB* survivait de manière similaire à la souche *wild type* (WT), des colonies plus petites furent néanmoins observées suivant l'infection. Les conditions endosomales (i.e. peu de nutriments et un pH acide) furent simulées afin d'évaluer leur impact sur la taille des colonies. Bien que le pH acide ne sembla pas avoir d'effet, la faible disponibilité en nutriments sembla impacter le mutant de la même manière que l'infection. De plus, de la microscopie à contraste de phase a permis de mettre en évidence un défaut de morphologie pour le mutant *ialB.* Suite à ces résultats, des souches de délétions furent ensuite conçues. Cependant, puisque la délétion de *ialB* ne fut pas possible, la seconde partie de ce travail se concentre uniquement sur Opp. Pour la souche de délétion, l'entièreté de l'opéron *opp* fut supprimée. Comparé à la souche WT, le mutant Δ*opp* a montré un retard de croissance lors de la culture en milieu riche. De plus, aucune différence avec la WT ne put être observée lors d'infection de macrophages. En conséquences, des investigations ultérieures devraient être menées afin, d'une part, d'explorer les différent rôles qu'Opp pourrait remplir ainsi que, d'autre part, pour comprendre pourquoi les mutants *ialB* et *opp* sont ressortis comme atténués lors du Tn-seq.

Mémoire de master 120 en biochimie et biologie moléculaire et cellulaire

Janvier 2017

Promoteur: Xavier De Bolle

University of Namur
SCIENCES FACULTY
Biology department secretary
Rue de Bruxelles, 61 - 5000 NAMUR
Phone: + 32(0)81.72.44.18 - Fax: + 32(0)81.72.44.20
E-mail: joelle.jonet@unamur.be - http://www.unamur.be

Downstream analysis of Tn-seq data and characterization of *ialB* and *oppB* genes from *Brucella abortus*

GODESSART Pierre

Summary

The genus *Brucella*, part of the alpha-proteobacteria, is composed of facultative intracellular pathogens. One of its member, *Brucella abortus* is the causative agent of the bovine brucellosis. A large library of *B. abortus* transpositional mutants was previously used to perform a time-resolved Tn-seq in macrophage infection, with the aim to unravel genes required for the infection fitness. Based on those results, this work focused on two genes reported as important at 2 h post infection in RAW 264.7 macrophages. One (BAB1_0491) is homologous to *ialB,* and the other (BAB2_0701) is part of an operon encoding an oligopeptide ABC transporter (homologous to Opp). While IalB had been reported to play a role for human erythrocyte parasitism in *Bartonella bacilliformis,* Opp seems to have a broad range of possible functions. The aim of this master thesis was to characterize their functions.

First, mutant strains by disruption of *ialB* or *oppB* were constructed and used to perform macrophages infection where the *ialB* mutant showed a decreased survival. If the *oppB* mutant survival was similar to the wild type (WT), it displayed smaller colonies that could be due to the infection process. Endosomal conditions (i.e. nutrient depletion and acidic pH) were then tested for the formation of this small colony phenotype. The acidic pH did not seem to have an impact, but the nutrient depletion appeared to have the same outcome than the infection. Also, phase contrast microscopy of the *ialB* mutant revealed a morphology impairment. Based on those results, deletion strains were designed. Because the *ialB* deletion was not possible, the second part of this work is solely based on Opp for which a deletion of the complete *opp* operon was generated. The Δ*opp* mutant displayed a growth delay in rich medium, compared to the WT strain. The Δ*opp* mutant behaved similarly to the WT strain in macrophage infection. Also, no morphological impairment could be observed for the Δ*opp* strain. Further investigations are required to explore the roles that could be carried out by this oligopeptide transporter, and to understand why *ialB* and *opp* mutant were scored as attenuated in the original Tn-seq experiment.

Master 120 in biochemistry and molecular and cellular biology thesis

January 2017

Supervisor: Xavier De Bolle

Acknowledgments

J'aimerai tout d'abord remercier mon promoteur, Xavier De Bolle, pour m'avoir accueilli aussi chaleureusement dans son équipe ; mais aussi pour sa disponibilité et pour toutes ces discussions remplies d'idées, de conseils et surtout d'une passion évidente pour la science.

Merci aussi à mon encadrant, Jean-François, à qui j'espère avoir montré que je ne foirerai pas et que je serai fort. Merci de m'avoir formé, inculqué tant de notions nécessaires au travail en laboratoire et donné de précieux conseils. Au-delà de l'aspect travail, merci pour ces nombreux fous rires bien qu'ils n'aient pas toujours eu lieu au bon endroit ni au bon moment.

Merci aux membres du jury, Karine Van Doninck, Emilie Bauwens, Arnaud Machelart et Francesco Renzi pour l'attention qu'ils ont porté et porteront à ce projet ainsi que le temps consacré à la lecture de ce mémoire.

Un grand merci à la Xa-Team, Katy, Mathilde, Vicky, Phuong et Kevin, pour votre bonne humeur quotidienne, vos conseils et votre aide. Katy, ne laisse pas le gnome prendre le dessus bien que ses apparitions soient toujours drôles à entendre. J'espère que tu retrouveras le temps de refaire des photos. Tu peux toujours compter sur moi. Mathilde, WESH ! J'avais pensé à d'autres choses, mais au final, cela les résume bien. Vicky, the "centri witch", thank you to have helped me to deal with these two weeks during the summer no man's land. Phuong, ta gentillesse te portera loin, j'en suis certain. Kevin, merci pour tous les conseils donnés et pour avoir participé à la résolu des déboires techniques rencontrés.

Merci à tous les membres de l'URBM pour maintenir cette ambiance de travail conviviale. Je tiens aussi à remercier les techniciens du laboratoire pour leur travail, Françoise, Aurélie et Mathieu, sans qui nous ne pourrions pas avancer comme nous le faisons. Sans oublier les GeMo que je remercie de nous donner la motivation d'arriver au bout de ces vendredis parfois bien longs.

Merci à Agnès, Sophie, Morgane, Sébastien et Denis sans qui ces cinq années d'études n'auraient pas été aussi riches en sorties, rires et grandes conversations. Mention spéciale à Denis, qui ne nécessite pas d'être développée, tu sais tout le bien que je pense de toi. A Agnès, je n'aurai pas pu penser à meilleure personne pour partager les craquages de la rédaction et partager ce bureau, ne lance PAS ce Nerf !

Merci à mon entourage familial pour m'avoir permis d'arriver là où j'en suis aujourd'hui et concrétiser ce que j'ai toujours voulu devenir, un scientifique (ou du moins, je l'espère !). Enfin, et pas des moindre, un gigantesque merci à Pauline qui m'aura accompagné tout du long de ces études et qui aura su partager mon enthousiasme, m'encourager quand le besoin s'en faisait sentir, me supporter dans les moments plus difficiles et surtout, d'avoir toujours cru en moi lorsque j'en doutais. Rien ne se serait aussi bien déroulé sans toi.

« Absence of evidence is not evidence of absence »

Martin Rees

Table of content

Abbreviations

aa	Amino acid
ABC	ATP-binding Cassette
aBCV	Autophagocytic *Brucella*-containing vacuole
BCV	*Brucella*-containing vacuole
CDC	Centers for Disease Control and Prevention
CFU	Colony forming units
CβG	Cyclic β-1,2-glucans
eBCV	Early *Brucella*-containing vacuole
EE	Early endosome
EEA-1	Early endosomal antigen 1
ER	Endoplasmic reticulum
ERES	Endoplasmic reticulum exit sites
gDNA	Genomic DNA
GPI	Glycosylphosphatidylinositol
iBCV	Intermediate *Brucella*-containing vacuole
LAMP-1	Lysosome-associated membrane protein 1
LE	Late endosome
LPS	Lipopolysaccharide
NGS	Next generation sequencing
NLR	NOD-like receptor
OD	Optical density
PAMP	Pathogen-associated molecular pattern
PBS	Phosphate buffer saline
PG	Peptidoglycan
PI	Post infection
PRR	Pattern recognition receptor
rBCV	Replicative *Brucella*-containing vacuole
T4SS	Type 4 secretion system
TD	Transmembrane domain
TE	Transposable element
VF	Virulence factor
WHO	World Health Organization
WT	Wild type

Species	Host preference	Virulence
Brucella abortus	Cattle	Moderate
Brucella canis	Dog	Mild
Brucella ceti	Cetacea	N/A
Brucella inopinata	N/A	N/A
Brucella melitensis	Sheep, goat	High
Brucella microti	Common vole	N/A
Brucella neotomae	Desert woodrat	N/A
Brucella ovis	Sheep	N/A
Brucella papionis	Baboon	N/A
Brucella pinnipedialis	Seal	N/A
Brucella suis	Pig	Moderate

Table 1 | Species of *Brucella*, their host specificity and their human virulence potential when applicable. The classical species are in black while the atypical species are in light grey. The host preference is not applicable for *B. inopinata* as it was isolated from a breast implant (Scholz *et al.*, 2010). N/A: not applicable

Introduction

Discovery

During the end of the 19th century, on Malta island, many British army soldiers were invalidated by an undulant fever associated with rheumatism as complication and a sometimes fatal undulant fever. To identify the cause of this so-called "Malta fever", the physician David Bruce was sent to Malta. In 1887, after a Gram staining, he observed a micrococcus isolated from the spleen of a deceased patient (Bruce, 1887). It was later named *Micrococcus melitensis* (renamed later *Brucella melitensis*) and confirmed as the brucellosis causative agent.

If several reports had already described the clinical aspects of the disease before *Brucella* discovery, it is hard to know when brucellosis was first recorded. Nevertheless, a 2009 study identified skeletal lesions on *Australopithecus africanus* remains that were most likely due to brucellosis (D'Anastasio *et al.*, 2009). If correct, this means that this illness is at least circa 2.5 Ma old. However, these assumptions are only based on osteological evidence, and even though very likely, these results lack molecular technics to identify the pathogen. Two genetic markers specific to *Brucella* (IS6501 and *Bcsp31*) were proposed to assess the presence of the bacteria. These markers were used successfully in a study based on skeletal lesions observed remains dated from the 10 to 13th century found in Butrint, Albania (Mutolo *et al.*, 2011). Therefore, as far as genetic clues are concerned, the oldest known case of brucellosis is dated from the middle age.

Phylogeny and host specificity

Since the discovery of *Micrococcus melitensis,* several other species have been identified. These species are grouped in the *Brucella* genus. The latter belongs to the alpha-proteobacteria and therefore, is part of the Gram-negative bacteria. This class includes several taxa among which some species are plants symbionts or plants pathogens such as *Sinorhizobium sp.* or *Agrobacterium sp.*, respectively, while other groups contain intracellular pathogens and commensals of animals, like *Bartonella* sp. and *Wolbachia* sp. (Ettema *et al.*, 2009).

The *Brucella* genus is divided into two parts: the classical and atypical species. The classical part comprises nine members: *B. melitensis*, *B. abortus, B. ovis*, *B. canis*, *B. suis, B. neotomae, B. ceti, B. pinnipedialis* and *B. papionis*. All these species seem to have diverged simultaneously (Wattam *et al.*, 2014). In the atypical species are found *B. inopinata* and *B. microti* that are different from the others in that they have a faster growth and seem more metabolically similar to the *Ochrobactrum* genus (Al Dahouk *et al.*, 2010). It should be noted that more species have been recently discovered in other organisms such as the frog (Eisenberg *et al.*, 2012, Fischer *et al.*, 2012 and Whatmore *et al.*, 2015) or the fox (Hofer *et al.*, 2012, Scholz *et al.*, 2016). Though close relatives with *Ochrobactrum*, *Brucellae* is a monophyletic genus and all its members are very closely related with a nucleotide identity of > 90 % (Whatmore, 2009). Nevertheless, one should be aware that new species of *Brucella* are continuously discovered as, for example, *B. vulpis* sp. (Scholz *et al.*, 2016) and therefore, their phylogeny is subject to changes.

As shown in Table 1, all the listed species have their own host specificity (exception made of *B. inopinata* that was isolated from a breast implant (Scholz *et al.*, 2010)). Concerning *B. abortus*, the species used in this work, it infects the cattle. However, it happens that the bacterium can infect other organisms. Regarding *B. abortus, B. melitensis, B. suis* and *B. canis*,

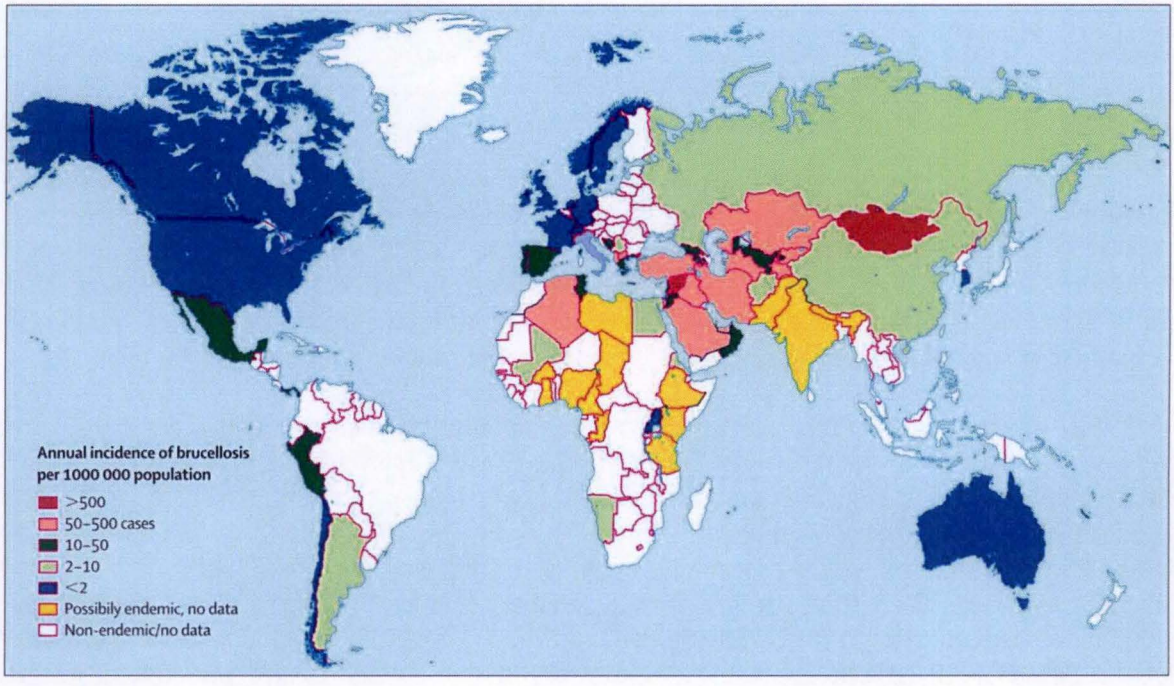

Figure 1 | Brucellosis worldwide distribution. As depicted above, brucellosis is still widely spread across the planet. However the number of countries where there is a lack of data is probably causing an under estimation of its prevalence (Pappas *et al.*, 2010).

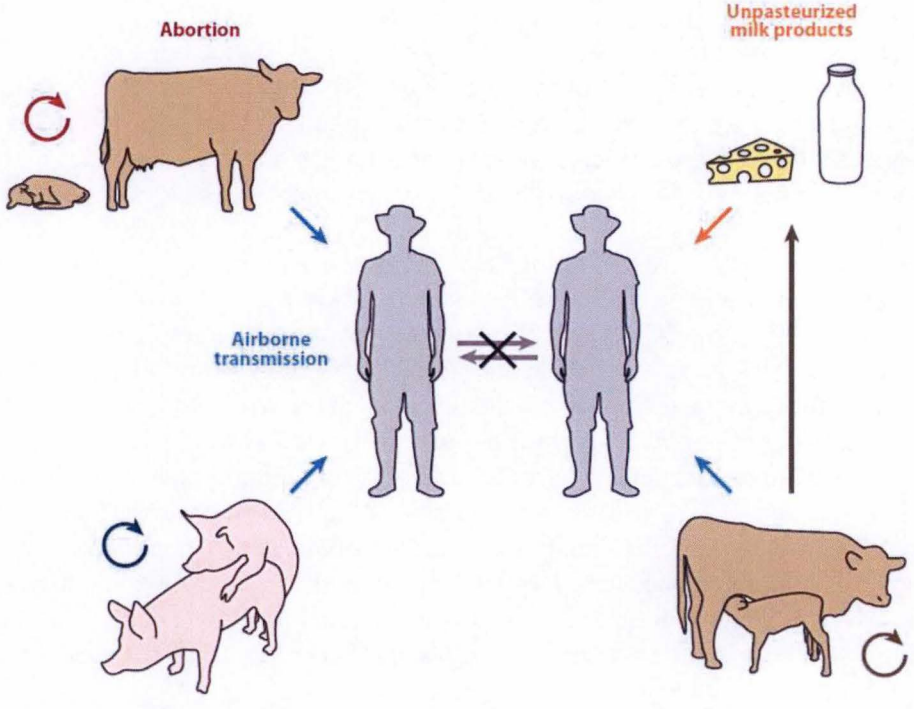

Figure 2 | *Brucella* infection routes. In the natural host, *Brucella* displays three infection routes: an airborne transmission ensured by the abortions, through mating or by offspring feeding. Regarding the human, airborne transmission is possible by aerosols produced during abortion or by close contact. The infection can also occur by the consumption of unpasteurized dairy products such as milk and cheese (Alturi *et al.*, 2011).

this other host can be the human (Atluri *et al.*, 2011; Galinska and Zagorki, 2013). Although human is considered as an accidental rather than a secondary host since it cannot spread the bacterium and thus, it represents a dead end when it comes to transmission. However, in some rare cases, such transmission has been observed (Mesner *et al.*, 2007).

Brucella and pathology

Epidemiology

With more than 500 000 new cases annually, brucellosis is considered as a major zoonosis across the world (Pappas *et al.*, 2006). Moreover, most affected countries are often emergent or underdeveloped where a reliable diagnostic is not always possible, meaning that the presence of the disease is probably underestimated. Brucellosis incidence varies widely between continents but also between countries as depicted in Fig. 1. Regarding Europe, several countries have been qualified of brucellosis-free while most of the Mediterranean countries, still endemic (Pappas *et al.*, 2006). However, this status should be considered carefully as it may only concern bovine, ovine and porcine livestock. Moreover, in 2012, a case of brucellosis has been identified in France, which was considered as bovine brucellosis-free since 2005 (Mailles *et al.*, 2012). In Belgium, which has also been granted with a bovine, ovine and porcine status (CODA-CERVA), a few cases of bovine brucellosis have been diagnosed in early 2010 (Fretin *et al.*, 2013). Also, the disease is widely present and endemic among wild boars (Grégoire *et al.*, 2012). Therefore this status does not mean that brucellosis is completely eradicated but at least that identified cases in the cattle are sporadic.

Transmission and pathology

In its natural host, *Brucella* can cause abortion in pregnant females and can lead to infertility in males. These consequences are due to its tropism for placental and reproductive tissues. To ensure its transmission, *Brucella* has three infection routes: through mating, *via* offspring feeding, or through abortion (Fig. 2). If the two first ways involve a direct contact with the source, the last one likely involves an airborne transmission. Indeed, the placenta is intensively infected with up to 10^{13} CFU.g^{-1} (Alexander *et al.*, 1981) while the infectious dose is as low as 10 to 100 bacteria per organism (de Figueiredo *et al.*, 2015). Consequently, it seems that the most frequent routes of infection are the mucosal membranes such as those present in the oral, respiratory and gastrointestinal tracts but also through the reproductive organs in the natural host only.

As a result, if one animal gets infected, it becomes a threat to the herd health. This high infection potential is the cause of the substantial brucellosis economic impact. Once infected, an onset of symptoms are exhibited by the host. Among them are found a recurrent fever, an enlargement of the lymph nodes, the spleen and the liver. Arthritis as well as gastrointestinal and neurological symptoms may also appear. If the host had to be immunocompromised, the bacteria could affect many other organs and even invade the central nervous system which would lead to the death (Moreno and Moriyón, 2006).

Humans can get infected through the airborne route following the exposure to the infected placenta, fluid and aborted foetus or through the consumption of unpasteurized dairy products (Fig. 2) (Atluri et. al., 2011; Galinska and Zagorki, 2013). Regarding the human acute brucellosis symptoms, it typically presents a strong undulating fever, headaches, muscular pains and gastrointestinal symptoms. If the disease remains untreated, a chronic infection can develop

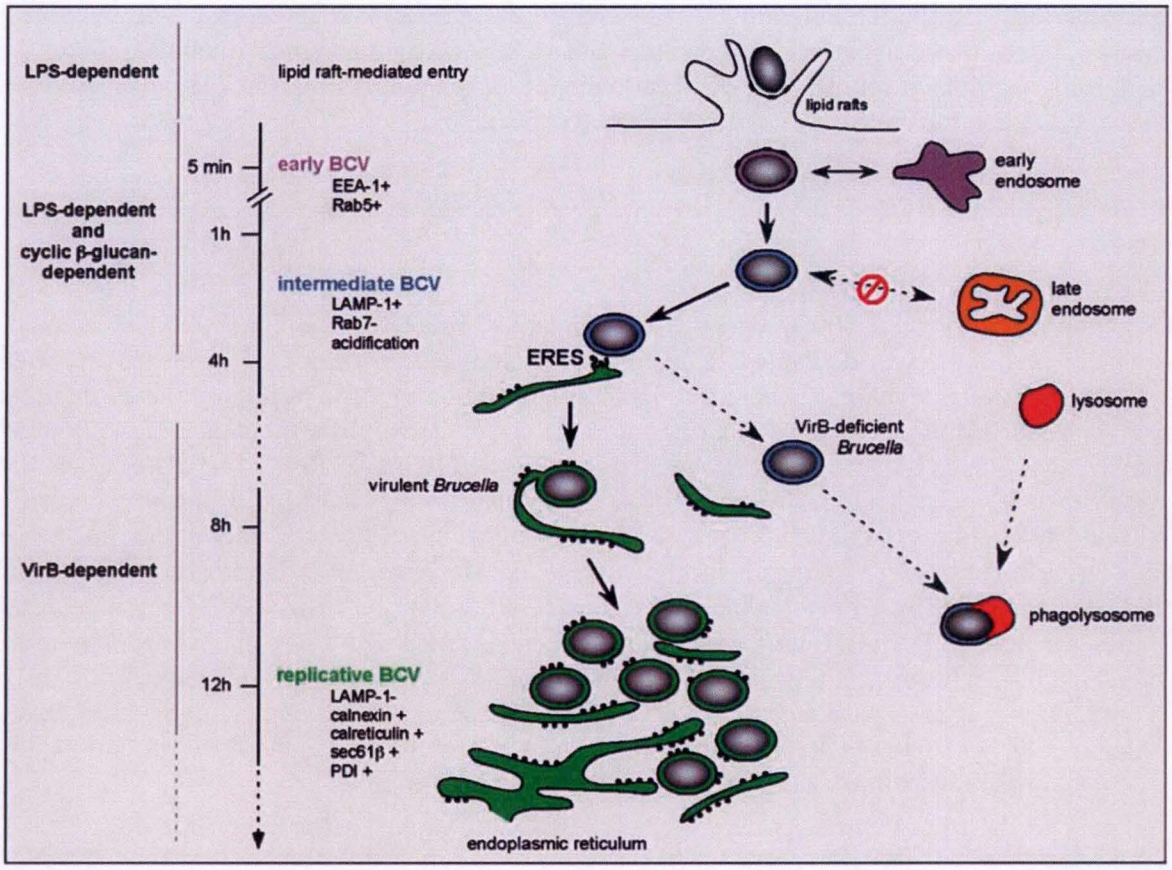

Figure 3 | *Brucella* intracellular trafficking in macrophages. After a lipid raft-mediated entry in a LPS-dependent manner, the bacteria is found in the eBCV (in purple). After transient interactions with the early endosomes (EE), the intermediate BCV (in blue) undergoes an acidification and acquires the LAMP-1 marker but no other late endosomal marker. As a matter of fact, the BCV avoids the interactions with both the late endosomes (LE) and the lysosomes, in part thanks to its cyclic β-1,2-glucans. The intermediate BCV (iBCV) then sustainably interacts with the ER exit sites (ERES) in a VirB-dependent manner leading to the formation of the replicative BCV. Bacteria lacking the VirB type IV secretion system cannot avoid the lysosome fusion (Celli, 2006).

and affect other organs. This will further give rise to arthritis, which is the most common complication, and in a few cases, encephalomyelitis and endocarditis. At this stage, the outcome can be the death of the patient (de Figueiredo *et al.*, 2015; Galinska and Zagorki, 2013).

Diagnosis and treatment

Currently, the brucellosis diagnostic is well established and is based on serology. These methods take advantage of the immunological response induced by the bacterial lipopolysaccharide (LPS). However, these methods can suffer from a lack of sensitivity or specificity. For example, it has been shown that similarities between the O-chain of *Brucella* and *Yersinia enterocolitica* can cause cross-reactivity which limits the specificity of some tests (Kittelberger *et al.*, 1995). In the end, the infection confirmation is brought by the isolation of the bacterium from the patient tissues (Moreno and Moriyón, 2006).

Regarding the treatment, it is often composed of two different antibiotics in a combination that can vary. According to the WHO (World Health Organisation) as well as the CDC (Centers for Disease Control and Prevention), a combination of doxycycline and rifampicin administration for six weeks is recommended. This therapy has the advantage to have a low rate of relapse.

Experimental models

Brucella being an intracellular pathogen, *in vivo* and *in vitro* models are required to achieve a better understanding of the bacterium. In pregnant ruminants, a study showed that *B. abortus* resides and replicates within the endoplasmic reticulum (ER) of the trophoblasts (Anderson and Cheville, 1986). The same localization was then observed in other non-professional phagocytes types such as the Vero cells[1] (Detilleux *et al.*, 1990a) or HeLa cells (Pizarro-Cerda *et al.*, 1998) as well as in professional phagocytes (Arenas *et al.*, 2000). Therefore, it suggests that the same infection process is observed in these *in vitro* models than in the natural host and they constitute suitable models for cellular infection studies.

In this work, RAW 264.7 murine macrophages were chosen as the model of infection. This choice was based on two main reasons: RAW 264.7 are professional phagocytes. That means that bacteria are more readily internalized which is more convenient to study the infection process and that secondly, trafficking inside a macrophage is more challenging for the bacteria. Another interesting aspect of the macrophages is that the brucellosis chronicity might rely on their infection (Celli *et al.*, 2003).

Macrophages infection

Even though *Brucella* intracellular trafficking in macrophages has still some grey areas, it has been rather well described during the last decade (Fig. 3). As for other micro-organisms such as Mycobacteria (Gatfield and Pieters, 2000), *Brucella* entry into macrophages is proposed to rely on interactions with the lipid rafts[2]. Besides, the lipid rafts disruptions significantly reduce *Brucella* early survival, suggesting a dual role (i.e. entry and early survival) for them (Naroeni and Porte, 2002). Nevertheless, it should be kept in mind that these effects may be indirect. It was also reported that rough bacteria are more phagocytised but are also eliminated

[1] Kidney epithelial cells isolated from the African green monkey *Cercopithecus aethiops*.
[2] The lipid rafts are composed of lipids (such as cholesterol), glycolipids and GPI-anchored molecules assembled into a raft (Anderson, 1998).

faster than smooth[3] strains (Jiménez de Bagüés *et al.*, 2004). Combined with the findings that these mutants enter into the cell in a lipid raft-independent manner (Porte *et al.*, 2003), this is consistent with an importance of both the O-chain and the lipid rafts for the early survival into the host cell.

After the entry, the bacteria are found in a membrane-bound compartment called the early *Brucella*-containing vacuole (eBCV), a single bacterium-containing compartment. The survival of *Brucella* mainly depends on its ability to avoid prolonged interactions with the endocytic pathway and more especially to avoid the lysosome fusion. Yet, the BCV maturation requires a transient interaction with the early endosome (EE) that goes along with the early endosomal antigen 1 (EEA-1) EE markers acquisition. Early stages of the BCV maturation involve the vacuole acidification which seems essential for later survival (Porte *et al.*, 1999). Concomitantly, the vacuole acquires the LAMP-1 glycoprotein, which is a typical marker of the endocytic pathway. However, the absence of other late endocytic compartment markers such as Rab7 or Cathepsin D, suggest that the intermediate BCV is able to segregate from the classical pathway to its replication niche (Celli *et al.*, 2003).

One of the mechanisms known to be involved in this segregation relies on the cyclic β-1,2-glucans (CβG). Indeed, when the CβG synthetase gene is mutated, the bacteria is unable to avoid the fusion with the lysosome (Arellano-Reynoso *et al.*, 2005). While in other α-proteobacteria these compounds have been found to be osmoregulated, it is not the case in *Brucella*. Their function is rather related to their ability to extract the cholesterol from the eukaryotic membranes and therefore, to disrupt the phagosomal membranes lipid rafts. These lipid rafts are thought to be necessary for the signalling in the phagosome maturation. In this, interfering with the pathway signalling would be crucial to avoid the fusion with the lysosome (Dermine *et al.*, 2001).

As said previously, the early and rapid BCV acidification is critical for the late survival. The expression of the *virB* operon, coding for the type IV secretion system (T4SS), is induced by an acidic pH as well as a temperature of 37°C and a poor nutritive environment (Boschiroli *et al.*, 2001). If *Brucella* T4SS mutants have been shown to equally survive during the early infection compared to the WT strain, they are later killed, highlighting their inability to avoid the lysosomal fusion for prolonged periods (Celli *et al.*, 2003). The *virB* operon is, therefore, essential to reach the bacterial replication compartment. Regarding the effectors, i.e. the proteins translocated through the T4SS, few have been identified and little is known about their functions or their mechanisms of action, except that they are thought to modulate the BCV trafficking (Myeni *et al.*, 2013).

The replication niche (or rBCV) results from sustained interactions with the endoplasmic reticulum leading to the formation of an ER-derived organelle characterized by ER markers but a loss of LAMP-1. These dynamic interactions take place at sites where ER membrane fusions and fissions happens (Celli *et al.*, 2005). Such domains are called the endoplasmic reticulum exit sites (ERES) and are the place where vesicles travelling between the ER and the Golgi apparatus are formed or engulfed. The BCVs sustained interactions with these exit points will somehow allow the bacteria to reach the ER or an ER-like compartment, by a mechanism that is currently unclear. Eventually, these interactions with the biosynthetic/secretory pathway place the bacteria in a nutrient rich environment where the proliferative phase can start, around 6 to 12 h after its entrance.

[3] A strain is qualified of "smooth" when its LPS comprises the O-chain. On the contrary, the term "rough" is used when this O-chain is missing.

Spreading from a cell to other cells would constitute a major step of *Brucella* infectious cycle. It has been reported that by 48 h post infection (PI) and, therefore, after the replicative phase, one or many bacteria can be observed in multi-membranes structures likely to be autophagosomes. These structures, consequently named aBCVs (autophagic *Brucella*-containing vacuole), were also found to be responsible for bacterial release and cell-to-cell spread (Starr *et al.*, 2012). These findings suggest an important role of these autophagosome-like BCVs in the completion of *Brucella* infectious cycle.

Vaccines

If antibiotics are used to cure human brucellosis, this treatment is not adapted for animals. Indeed, it usually requires the use of two different antibiotics at high doses for an extended period and in some cases, the individual remains infected (Ariza *et al.*, 1995). Therefore, due to these constraints and besides systematic slaughtering of the infected herds, it seems that the solution should not cure the disease but rather prevent it. In this regard, vaccines are the most efficient way to decrease the animal brucellosis and, consequently, the human incidence. Up to date, there is still no gold standard in the sense that none of the existing vaccines achieves a sterilizing immunity against *Brucella*. Besides, they also suffer from several drawbacks.

The most effective vaccine and the reference in term of efficiency is the live S19. It was developed from a spontaneously attenuated *B. abortus* strain 19 mutant. Even though it is the most efficient, it does not provide a full immunity and has an efficacy estimated at approximately 70% (Lubroth *et al.*, 2007). However, this is a smooth strain and the vaccinated animals develop persistent antibodies jeopardizing *Brucella* diagnosis. Moreover, it remains abortive and fully virulent for humans. To circumvent the issues inherent to the S19 vaccine, the live RB51 was introduced in 1996 (Yang *et al.* 2013). Contrary to the S19, this is a rough mutant derived from *B. abortus* 2308, and it should not interfere with serological tests for the diagnosis. It is also safer regarding the abortive potential while it is still virulent to humans, which is, of course, a major concern. Moreover, this mutant is naturally resistant to rifampicin, which constitutes a major drawback as this drug is one of the most efficient antibiotic against human brucellosis. Other live vaccines, such as the *B. melitensis* strain Rev-1, have been developed but are not discussed here as this work focuses on *B. abortus*. Studies have tried to modify the vaccines presented above but so far, none of them has achieved a better protection than the S19 and RB-51 vaccines Goodwin *et al.*, 2016).

Of course, to bypass the problem of residual virulence of attenuated strains and the inability to distinguish vaccinated and infected animals, subunits vaccines could be used as they only contain an antigen and not a whole organism. Due to the high percentage of homology among the *Brucella* genus, these vaccines have the advantage to be efficient against multiple species. The main reason why they are not broadly developed and used is they do not reach the protection percentage of the live vaccines (Yang *et al.*, 2013).

Consequently to this absence of a gold standard, research has to be continued. One approach is to study virulence factors (VFs). These are molecules that are essential for the bacterial pathogenicity as they allow the pathogen to deal with every aspect of the host infection. Some of them are mentioned above, in the *Macrophage infection* part, such as VirB. Those aspects include the interactions with the immune system, the ability to reach the replication niche or the acquisition of nutrients. Hence, their field of action is broad and reflects their diversity as well as the challenge representing their identification. Nevertheless, the

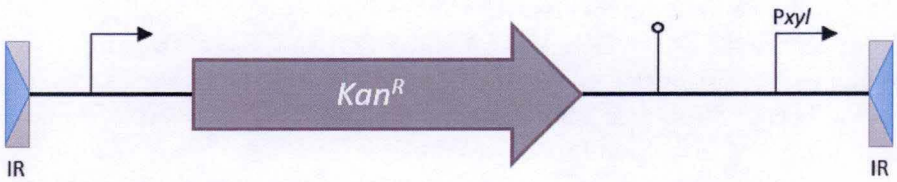

Figure 4 | Schematic representation of the mini-Tn*5*. It features a kanamycin resistance gene used for selection, and therefore a promoter that is dedicated to its expression as well as a hairpin after the Kan^R that acts as a transcriptional terminator. It also harbour a Xylose promoter that is constitutively active in *B. abortus*, preventing polar effects on downstream genes.

identification of a crucial VF is of important matter as it could represent a new drug target or it could lead to the engineering of a new vaccine candidate.

The approach

During the last decades, the rapid progress made in the sequencing area have led to the publication of a substantial number of bacterial genomes. However, the knowledge of the genes function has not followed this exponential progress. It is even said that if one had to sequence a new organism genome, the percentage of genes associated with a known function would be similar to that obtained as far as a decade ago (Kasif and Steffen, 2010).

Nevertheless, the massive genomes publication has led to an unprecedented use of transposition. Indeed, while the transposons had already been described, having complete genomes sequenced allowed to link a transposon-mediated gene disruption (i.e. a genotype) to a phenotype. The transposons, also called transposable elements (TEs), have the ability to move inside or between genomes. Up to now, many different types of TEs have been described and are categorized into two classes. Contrary to the class 2, the class 1 members require a reverse transcription to move and are thus qualified of retrotransposons. However, they will not be discussed any further as the Tn-seq only make use of the class 2 transposons, also called DNA transposons. The latter classically possess a transposase coding gene. This protein excises the genetic element from its position and allows its insertion somewhere else *via* a conservative mechanism called "cut and paste" or the replicative "copy and paste". In addition of this gene, they also contain inverted repeats at both ends that are recognized by the transposase for the sequence excision (Pray, 2008).

While this is the traditional structure of a transposon, those used in a research context have been adapted for the laboratory use. The main modification is the rearrangement of their functional elements to obtain shorter elements and are therefore labelled "*mini-transposons*" (de Lorenzo *et al.*, 1998). The mini-transposons are also characterized by the lack of transposase gene between the two inverted repeats (this gene is elsewhere on the the transposon-containing plasmid) and by the presence of an antibiotic-resistance marker. Most studies requiring transposon mutagenesis have used either mini-Tn*5* or mini-mariner transposon derivatives. While the Tn*5* originates from bacteria, the mariner comes from the eukaryotes (Barquist *et al.*, 2013). However, the most significant difference between both is also the disadvantage of the mariner: it requires a TA dinucleotide in the integration site (Lampe *et al.*, 1998). On the contrary, the Tn*5* does not have any strong hot or cold spot even though it has a slight preference for GC-rich sequences.

Although the transposon mutagenesis represented a breakthrough in functional genomics, its use remained limited. Indeed, studies reporting TEs usage in *Brucella* for VFs identification only had a mutant library of a few thousand to dozens of thousands of mutants (Wu *et al.*, 2006, Kim *et al.*, 2012). With a *Brucella* genome size of about 3.3 Mb, this is far from genome-wide investigations. Besides, due to the sequencing techniques available at that time, one could only focus on a relatively small number of genes (Wu *et al.*, 2006). Those elements considered, the advent of the massively parallel sequencing has constituted a real game changer allowing significantly larger mutants library and transposon insertion site identification.

In this respect, a technique called "*Tn-seq*" was presented in 2009 (van Opijnen *et al.*, 2009). It combines a saturated transposon mutagenesis and the next-generation sequencing (NGS) methods and the principle will be developed in details in the next section. The main

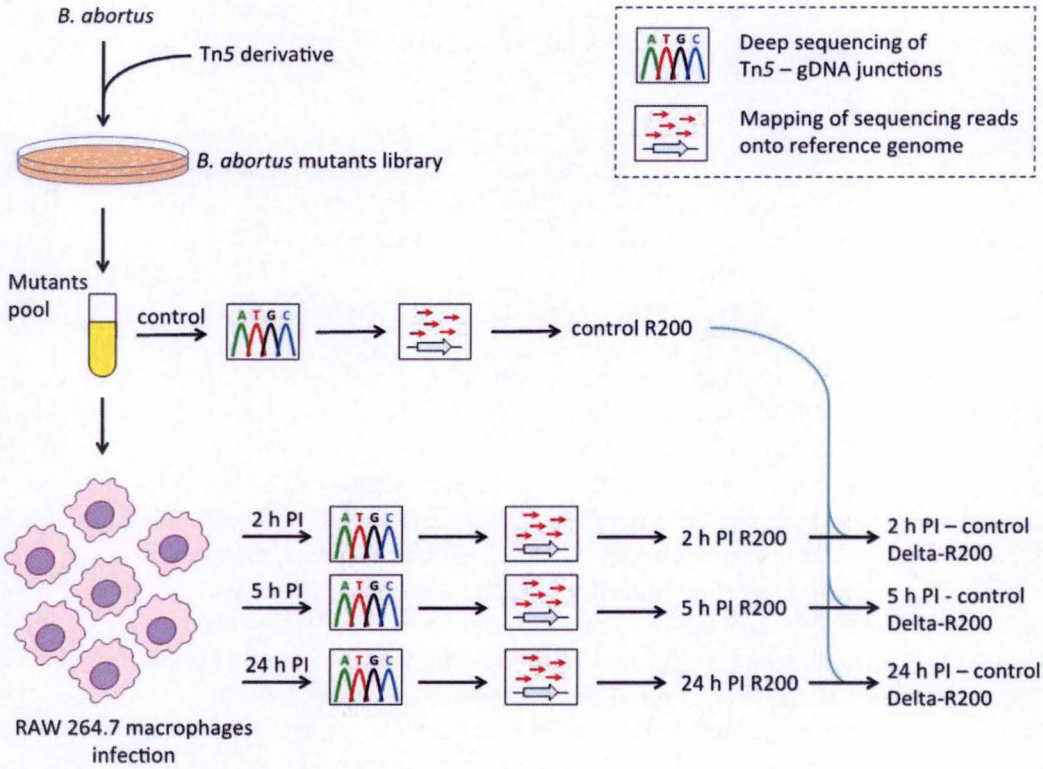

Figure 5 | Tn-seq schematic protocol. First, a *Brucella abortus* mutants library is generated with a mini-Tn*5* transposon. Once obtained, all the mutants are pooled together and this pool is divided in two parts. The first part is used as a control; the genomic DNA (gDNA) is sequenced at the Tn*5* junctions then, the reads are mapped onto a genome and the R200 values are calculated (see Fig. 6). The remaining part of the pool is then used to perform three RAW 264.7 infections. Bacteria are retrieved from the macrophages at 2 h, 5 h and 24 h post infection. As for the control, the gDNA is sequenced, the reads are mapped and the R200 values calculated. In order to obtain the genes only essential during the infection, the data from the control are subtracted from the three time point data *(Courtesy of J.-F. Sternon)*.

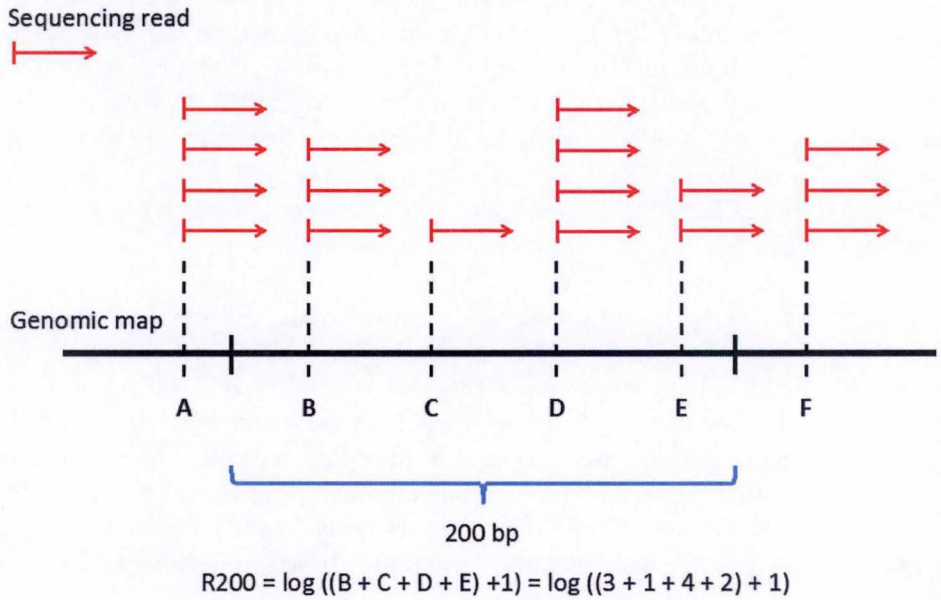

Figure 6 | R200 calculation principle. The R200 consists in counting the number of transposon insertion sites into a 200 base pairs window on the genomic DNA +1, then to take the base 10 logarithm of this number. The window is then moved 5 base pairs further and the calculation is repeated. The window is moved like that until it has covered the whole genome *(Courtesy of J.-F. Sternon)*.

advantages of this technique are that it can highlight relationships between a phenotype and the genotype as the transposon insertion will disrupt the gene and prevent its normal expression. Moreover, it applies to a broad range of species. Consequently, when used in infection conditions, the Tn-Seq has the ability to constitute a list of VFs candidates that then need to be characterized.

In order to identify genes necessary for the growth on rich medium and during the RAW 264.7 infection in *Brucella abortus*, a Tn-seq experiment was conducted at the University of Namur, in Xavier De Bolle's team (URBM/MBRU – microorganisms biology research unit) by Jean-François Sternon.

Tn-Seq

Regarding the Tn-seq experiment conducted by Jean-François Sternon, a mini-Tn*5* was used. As shown in Fig. 4, its main features are a kanamycin resistance gene and a Xylose promoter pointing outwards. The latter is proposed to drive an expression downwards the transposon insertion site and thus limit the polar effects of Tn*5* insertion. As said previously, this transposon type has a small bias for GC-rich sequences. However, due to the high insertion densities obtained with this mini-Tn*5*, this does not have a strong impact on the data and their analysis (Barquist *et al.*, 2013). The delivery plasmid was a pXMCS2 that harboured the transposase gene that has been modified to have an enhanced activity. Additionally, a *bla* gene, conferring the ampicillin resistance, is also present on the backbone of the plasmid.

As depicted in the schematic protocol representation (Fig. 5), a mutant library was constructed by conjugating an *Escherichia coli* containing the mini-Tn*5* plasmid with *B. abortus* 2308[4]. This library was made in such a way that a theoretical frequency of about one transposon every base pair (*i.e.* 3.10^6 mutants) was reached. Subsequently, all the mutants were mixed to obtain a homogeneous pool. Following this, the pool was divided into two parts. The first half was kept as a control of the genes already essential for the growth on a culture media. The second half was then used to proceed to the infection of RAW 264.7 macrophages. As explained above in the *Macrophage infection* section, bacteria undergo several challenges and different types of environments that take place at various times post infection. Due to this diversity, three time points (2 h, 5 h, and 24 h PI) were chosen to highlight the differences in gene essentiality along the infection process. After these time intervals, bacteria were extracted from the cells, grown on rich medium and as for the control condition, their genomic DNA (gDNA) was extracted.

The gDNA samples were then sequenced at their junctions with the Tn*5* and all the generated sequencing reads were mapped onto a reference genome. However, the generated data sets were raw and not easily analysable with the bare eye. Consequently, a simple computing was established to facilitate the reading. A score was named R200 and represents the transposon insertion frequency. Basically, it consists in the count of the insertions number per site plus one, that one can count in a 200 pb window and to take the base 10 logarithm of this number (Fig. 6). This window was then slid 5 bp further along the whole genome. This resulted in smoother graphics as shown in Fig. 7, which were more suitable to the analysis. Also, this notion was essential to determine essentiality as a gene was considered as such if it had a least one R200 equal to zero. The last step in the data treatment process was to subtract the control data to each infection data set, generating ΔR200 values that are negative if a

[4] On some bioinformatics website, this strain cannot be found unless under *Brucella melitensis* biovar Abortus 2308 which is a synonym. Nevertheless, this strain is part of the *abortus* and not of the *melitensis*.

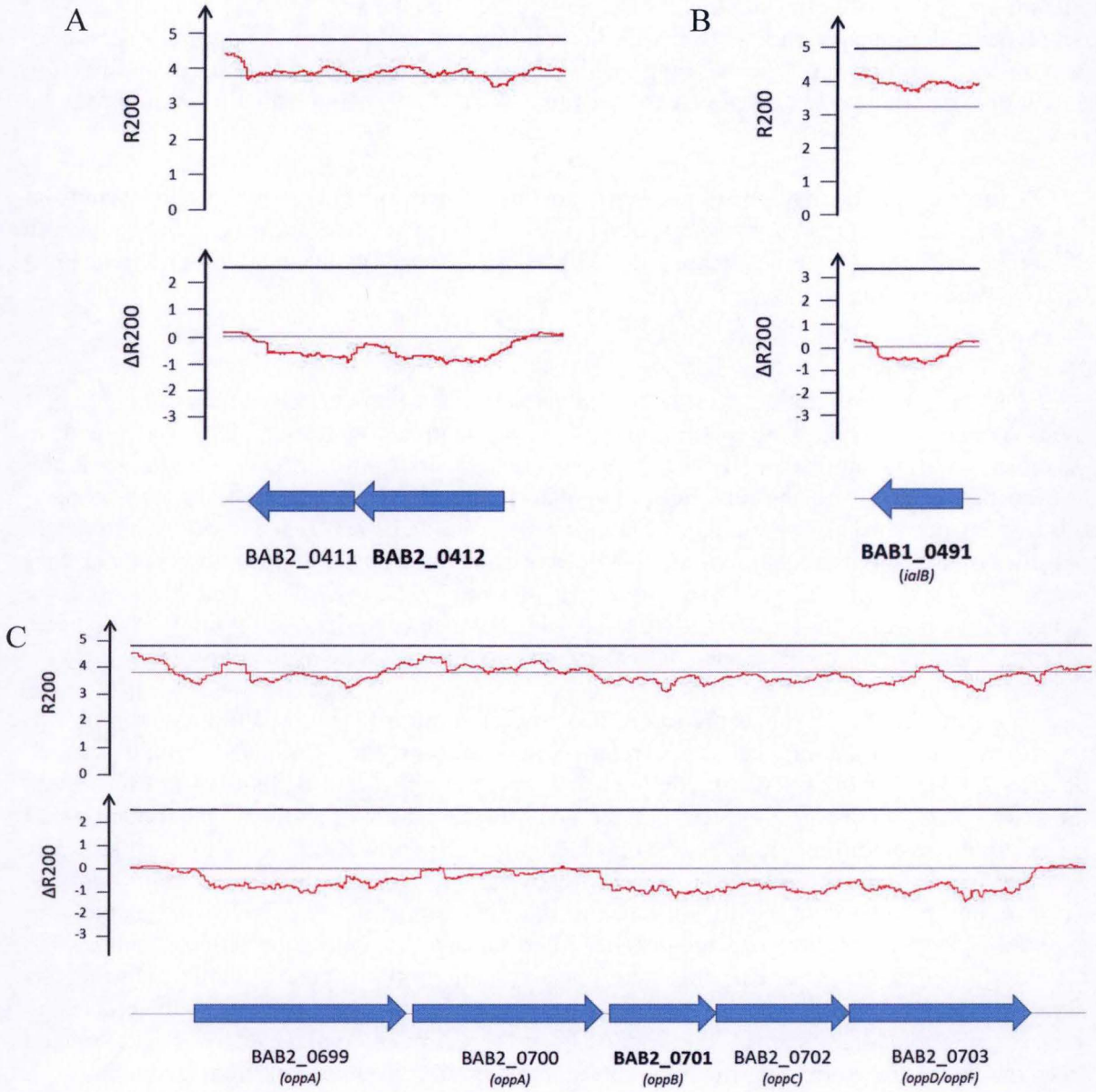

Figure 7 | Tn-seq profiles of the three candidates (in bold): BAB2_0412 (A), *ialB* (B) and *oppB* (C). Each sub-figure follows the same pattern. The upper graph represents the control condition and the lower, the 2 h PI time point. The Y axis indicates the R200/ΔR200 values and the X axis, the genome map. The upper graph possess two straight lines; the light grey is the chromosomal mean transposon insertion number and the dark grey represents the maximum insertion number observed. Note that the two chromosome do not have the same transposon insertion values. On the lower graph, the dark grey is still representing the maxima but this time, the light grey line is centred at zero as this graph represents the delta of control and infection data (ΔR200). Therefore, when the red line (representing the delta between the control and the time point at a site) is below the light grey line that means that less mutants with an insertion at that site than the control value are observed, suggesting that a gene is important for a given condition.

particular set of mutants is attenuated. This action allowed to remove all the genes that were already essential for the growth on a plate and left only the genes that stood out at the different time points (Fig. 6).

The Tn-seq results will only briefly be discussed as, despite being based on them, this master thesis project occurred once Tn-seq data were analysed. Out of 3,419 predicted genes of *Brucella*, 14.4% (*i.e.* 491 genes) stood out as essential. However, these genes are not distributed equally on the two chromosomes (Chr I; 2.1Mb and Chr II; 1.2Mb). The first chromosome harbours 429 out of 491 essential genes, or 19.2% of its encoded genes while the second chromosome only has 62 essential genes, so 5.2%. This is not surprising considering that the Chr. II has been hypothesised as a stabilized megaplasmid (Halling *et al.*, 2005).

Following the experiment described above, two other Tn-seq were performed in the URBM. While the same mini-Tn*5* as in the original experiment was used to generate the mutant library, other parameters were changed.

The first alternative was also studying the essential genome of *B. abortus* but to this purpose, JEG-3 human trophoblasts were used. This choice of cells is also highly relevant as they constitute a primary cellular target in the natural infection process. However, only one time point (5 h PI) was set. The reason is that *Brucella* seems to have a different behaviour regarding its growth whether it is in trophoblasts or macrophages. In macrophages, *Brucella* seems to undergo a kind of dormancy as it only resumes its growth around 8 h PI (Deghelt *et al.*, 2014). Nevertheless, in trophoblasts, it seems more complex because a phase of growth is detectable at the single cell level, but no daughter cells are generated for several hours of infection, suggesting that growth is arrested later compared to macrophages. The growth is resumed later during the cellular infection. Therefore the aim of this Tn-seq is to gain new insights into the mechanisms regulating these differences.

Concerning the second Tn-seq, both the strain and the experimental model were different as mice were infected with *B. melitensis*. Also, the protocol followed was not the same than previously; after the library construction, bacteria were recovered and underwent a second round of culture on a plate. Regarding the time points, the bacteria were also recovered 5 h after the infection.

Candidates

Among all the candidates revealed by the originally performed Tn-seq on RAW 264.7 macrophages, three were chosen to be the subjects of this work. This choice was directed by two main reasons. Firstly, and obviously, the three genes exhibit a fitness decrease in RAW 264.7 infection (Fig. 7). Secondly, genome annotation based on homologies with other species allowed to predict a function for each of them. Also, the three genes are issued from the 2h PI time point that was set to highlight the genes required for adhesion, entrance or early survival.

BAB1_0491

BAB1_0491 is a 198 amino acids (aa) long encoding gene. Thanks to bioinformatics analyses, a signal peptide cleavage site was found between the 27th and the 28th amino acid using the *SignalP* program (Peterson *et al.*, 2011). This putative signal peptide has then been identified as an export signal by the *PSort* program (Yu *et al.*, 2010) placing this protein in the periplasmic compartment. Based on the homologies, this gene is annotated as an invasion protein. However, the term "*invasion*" is vague as it could reflect the gene importance at

different levels of the infection such as the adhesion, the entry or the early survival. According to a CD research (i.e. the detection of protein domains by homology) from the NCBI server, part of the sequence is found homologous to the *invasion-associated locus B* (IalB) with both a high identity percentage (89.86%) and a strong E-value ($2.52x10^{-50}$). Accordingly to this homology, BAB1_0491 will be renamed *ialB*[5] for the rest of this work.

While the *ialB* annotation can be found in many other α-proteobacteria, few studies have been investigating it in the literature. Besides, all these studies are performed in *Bartonella bacilliformis* where it was first identified (Mitchel and Minnick, 1995). Nevertheless, the findings in this bacteria can be relevant for *Brucella* as they are closely related (Willimas *et al.*, 2007). Moreover, even if erythrocytes are not commonly cited among the niche of infection, it has been reported that *B. melitensis* can invade and persist in erythrocytes (Vitry *et al.*, 2014). After the *ialB* identification, the encoded protein was reported as a virulence factor. Indeed, the deletion of *ialB* resulted in a substantial decrease of bacterial adherence and invasion of human erythrocytes (Coleman and Minninck, 2001). Two years later, it was reported by the same team that *ialB* level of expression was significantly higher in acidic conditions but also upregulated when at 37°C (Coleman and Minninck, 2003). Unfortunately, since then, no other studies aiming to the further characterization of IalB can found. Figure 7B represents the mutants' fitness in the control and the 2 h PI conditions obtained in the original Tn-seq. As shown, insertions in this region do not seem to affect the growth on rich medium. However, this gene becomes essential once in infection as depicted by the decrease of insertions that covers the whole open reading frame. Consistently, the same pattern of essentiality is observed at 5 h PI in trophoblasts.

BAB2_0701

BAB2_0701 is a 307 aa long encoding gene and as depicted in Figure 7C, is part of a 5 genes operon. Regarding homologies, it is predicted as part of an ATP-Binding Cassette (ABC) transporter and more specifically as one of the two permease transmembrane domains (TD). Homologies associate this gene to *oppB* which is part of the *opp* (for oligopeptides) operon from *E. coli*. Consequently, to simplify the understanding of the rest of this work, BAB2_071 will be renamed *oppB*. Regarding the transporter architecture, it follows the classical ABC transporter composition (Biemans-Oldhinkel *et al.*, 2006). Indeed, it has two transmembrane proteins (BAB2_0701 and BAB2_0702, respectively OppB and OppC) and while the *opp* operon has two nucleotide binding domains (OppD and OppF), only one (BAB2_0703) is present here (Dawson *et al.*, 2006). Concerning the two other genes, BAB2_0699 and BAB2_0700, they are homologous to OppA which is a soluble periplasmic substrate-binding protein. While present in both Gram-positive and Gram-negative bacteria, the transporter displays dissimilarities such as the anchorage of OppA in the cytoplasmic membrane or to the TDs (Biemans-Oldhinkel *et al.*, 2006).

It is known that this system is able to transport a large variety of peptides (Payne *et al.*, 1994). Due to this versatility, the Opp transporter is involved in many mechanisms such as the nutrient uptake, the cell wall recycling in *E. coli* and *Salmonella typhimurium* (Goodell and Higgins, 1987) or quorum sensing in *Bacillus subtilis* sporulation (Rudner *et al.*, 1991). Concerning nutrients uptake, it has been reported that the intracellular survival of *Listeria monocytogenes* in macrophages required OppA as it allows the intracellular peptides

[5] It should be noted that along this work, genes will always be written in small, italics with only the last letter in capital (e.g. *ialB)* and the proteins will be written in roman with the first and the last letter in capital (e.g. IalB). Protein complexes will be written with in roman with the first letter in capital (e.g. Opp).

internalization that will ultimately be used as nutrients (Borezee *et al.*, 2000). In *Clostridium difficile*, a Gram-positive, it has been shown that the import of nutrients through this ABC transporter inhibits the sporulation. The same study also reported a hypervirulence in transporters mutants, but the mechanisms of action are still unclear and require further investigations (Edwards *et al.*, 2014). On the contrary, an attenuated virulence in mice was reported in *Moraxella catarrhalis*, a Gram-negative bacteria. According to the authors, this is due to an impairment in their ability to persist in the respiratory tract, which constitutes its natural niche (Jones *et al.*, 2014). These examples reflect the role diversity of the Opp system in bacteria. As for the *ialB*, the Tn-seq operon profile shows an attenuation (i.e. a fitness decrease) for *oppB* during a macrophage infection (Fig. 7C). Interestingly, only one of the two substrate binding protein is required during the infection. The rest of the operon stands out as essential with a low ΔR200 value.

BAB2_0412

According to the annotations, this 316 aa gene has no known function yet. However, running a BLAST against its sequence allows to identify a putative conserved domain, TauE, which is an inner membrane sulphite exporter. As represented in Fig. 7A, it is located next to another gene, BAB2_0411 which exhibits the same attenuation pattern. The sulphite exporter function may not seem relevant for the bacteria virulence. However, it has been shown that sulphite can be oxidized by hydrogen peroxide. This results in the release of sulphate and water (Hoffmann *et al.*, 1975). In the light of the infection process, such a function could help the bacteria to deal with the H_2O_2 generated by the infected macrophage. Nevertheless, due to reasons that will be developed later, it was rapidly decided to focus on the two other genes.

Objective

The objective of this master thesis was to try to characterize genes identified as essential for survival in RAW 264.7 macrophages in a previous Tn-seq experiment performed within Xavier De Bolle's team. In this respect, the project was divided into two parts. First, disruption mutants were designed to quickly assess the respective mutant potentials as attenuated strain. These disruption mutants were used to infect RAW 264.7 macrophages to confirm the Tn-seq observation, i.e. their attenuation. Then, to test hypotheses related to the genes functions, a set of different experiments were performed. Following the outcome of the first part, the second one consisted of the construction of deletion mutant strains. Such strains would allow to confirm the results obtained with the disruption mutants and then to continue the investigation of the different genes.

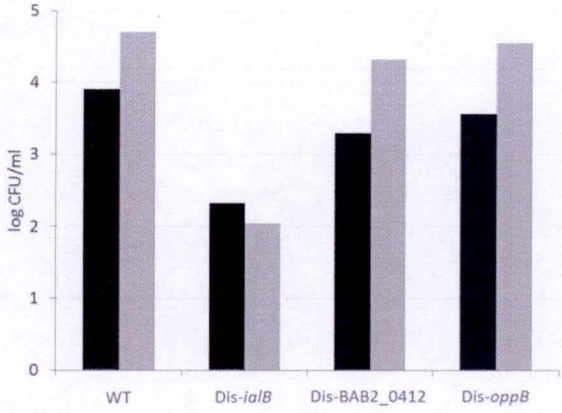

Figure 8 | Number of CFUs (logarithmic scale) for the WT strain and the three disruption mutants after a 2 h infection in RAW 264.7 macrophages. In black, bacteria from an overnight culture and in grey, from resuspended colonies. Only the *ialB* disruption mutant exhibit a decrease in term of CFU numbers in both cases. Even though the experiment has been performed three times, the first obtained results were too different compared to the two other data set than to use any statistical test, this explains the absence of error bars.

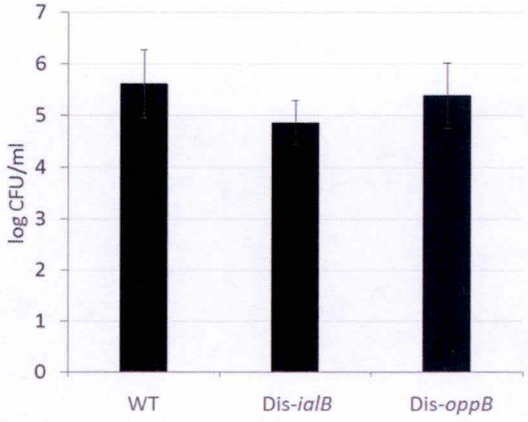

Figure 9 | Number of CFUs (logarithmic scale) for the WT strain and two disruption mutants (Dis-*ialB* and Dis-*oppB*) after a 24 h infection in RAW 264.7 macrophages. Error bars represent the standard deviation. Compared to the WT, the Dis-BAB1_0491 has a slight decrease but this has no statistical meaning. Regarding the Dis-BAB2_0701, no difference can be observed as for the 2 hours infection.

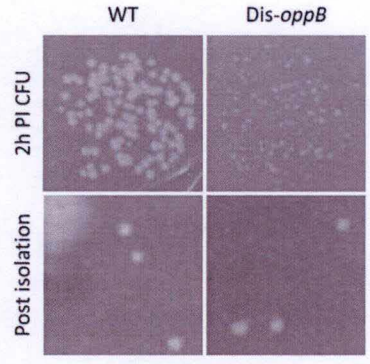

Figure 10 | Small colony phenotypes of the *oppB* disruption mutant. On the upper part, the WT and the mutant strain colonies plated after a 2 h infection in RAW 264.7. On the lower part, colonies were isolated and grown during three days. This restored the WT phenotype for the mutant.

Results

Disruption mutants

To confirm the Tn-seq results and to assess the candidates' potential interest, disruption strains were designed. This was done by inserting a pNTPS plasmid within the middle of the coding sequence *via* a homologous region present in the plasmid. This insertion likely prevents the gene to assume its function. Also, this plasmid harbours a kanamycin resistance gene. Consequently, to keep it integrated into the bacterial genome, all the disruption strains had to be cultured and grown in the presence of kanamycin to generate a selection pressure.

Infection ability

First, a RAW 264.7 macrophages infection was performed to confirm the results obtained by the Tn-seq. As the three mutants exhibited a fitness decrease at 2 h PI, bacteria were extracted from the macrophages at this time PI. As shown in the results (Fig. 8, black bars), only the *ialB* disruption mutant exhibits a significantly lower number of CFUs while the two other mutants do not seem to show any difference when compared to the WT strain. In this experiment, bacteria used for the infections came from an overnight culture. However, in the Tn-seq, as shown in Fig. 5, colonies were retrieved from plates, pooled together and then used to perform the macrophage infections. Consequently, as the conditions were different, it was decided to do the RAW 264.7 infections with bacteria collected from colonies. Indeed, one could argue that the bacteria state could be different whether they were grown in liquid culture or on solid medium and this could impact their physiological state, and therefore the CFUs results. However, the same pattern of CFU was observed as previously: only the *ialB* disruption mutant showed a decrease while the other mutants had similar CFU numbers compared to the WT (Fig. 8, grey bars).Even though the above results showed no differences between the different strains, it was decided to perform a 24 h PI timing to assess whether or not an effect could appear at later times. Regarding the 24 h PI Tn-seq data (Fig. S2), the transpositional mutants' fitness decrease observed at 2 h PI is still present and follows the same tendency as shown in Fig. 7C. The results (Fig. 9) show a smaller difference for the Dis-*ialB* strain than previously observed. However, it should be noted that in one of the replicate, this strain seemed to exhibit a growth delay on plates, as the CFUs appeared one day later. Consistently with the above results, Dis-*oppB* showed no difference compared to the WT. Because these infection tests were performed later than the rest of the disruption mutants experiments, the BAB2_0412 mutant had already been put aside.

Surprisingly, even if the *oppB* disruption mutant had no decrease in term of CFUs, it did exhibit a different phenotype. When grown on plates, after the infection process, the colonies seemed much smaller than the WT strain (Fig. 10, upper part). Furthermore, once the colonies were isolated and spread again on a plate, the WT phenotype was restored (Fig. 10, lower part). As the mutants were plated on rich medium supplemented with kanamycin to guarantee the disruption plasmid integration, it was decided to assess the potential influence of kanamycin on colony size. In this respect, a simple experiment was set up: the strains were incubated 2 h in PBS (Phosphate Buffer Saline), then the WT strain was spotted as a negative control while the *oppB* disruption mutant was spotted on rich medium with or without kanamycin. As shown in Fig. 11, small colonies were observed in both mutant conditions. Because small colonies were observed in both mutant conditions, PBS incubation was thought to be a potential cause for the small colonies phenotype. Therefore, it was decided to incubate the mutant in parallel in 2YT and PBS during 2 hours. The WT strain was incubated in the same conditions as a control.

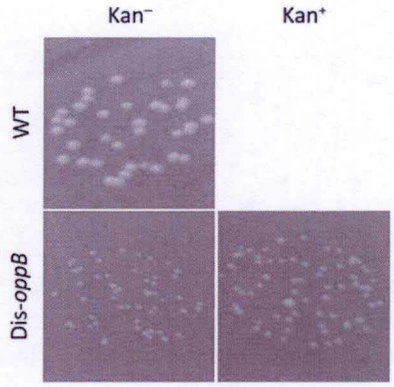

Figure 11 | Effect of kanamycin the *oppB* disruption strain. The WT strain (positive control) was grown without kanamycin (Kan^-) only. In both cases, with and without kanamycine (Kan^+ and Kan^-, respectively) the mutant exhibit small colonies. This likely excludes any effect of the kanamycin.

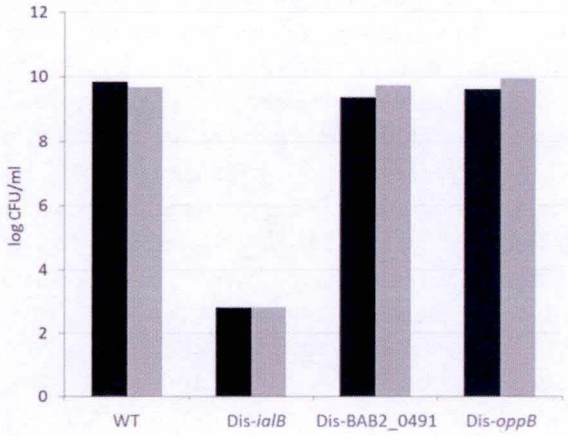

Figure 12 | Number of CFUs (logarithmic scale) for the WT strain and the three disruption mutants after a 2 h incubation in PBS (black bars) and in acidic PBS, pH 5 (grey bars). For Dis-*ialB*, it should be noted that this result is below the test sensitivity and could therefore not be accurate.

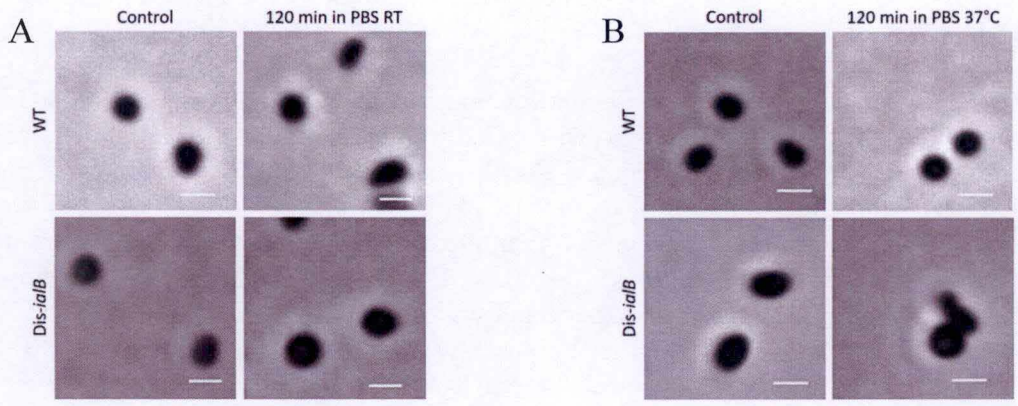

Figure 13 | Phase contrast microscopy before and after a 2 h incubation in PBS at (A) room temperature and (B) 37°C. In both temperature conditions, the WT strain maintain a normal phenotype before and after the PBS incubation. However, the mutant displays a lighter center. This is likely to reflect a swelling of the bacterium. Scale bars represent 2 µm.

As results, smaller colonies were observed after the incubation in PBS than in 2YT. It was also noticed that the amplitude of the colony size differences between the WT and the mutant strain was not constant and could vary from one experiment to another, thus complicating the experimental readout.

ialB mutant starvation sensitivity

As explained in the introduction, once the bacteria are uptaken by phagocytosis, their environment is thought to be rather hostile. Indeed, in the BCV *Brucella* is proposed to encounter several stress such as nutrients depletion and an acidic environment (Roop *et al.*, 2009). To mimic these conditions and assess their potential impact on the bacteria survival, PBS and acidic PBS (pH 5) were used to perform 2 h long incubations. According to the results (Fig. 12), patterns similar to those seen in infection results are observed. Thus the *ialB* mutant is sensitive to a short (2 h) incubation with PBS. Even though it appears that there is no difference between the nutrients deprivation and nutrients deprivation combined with an acidic pH for the *ialB* mutant, one should not jump to conclusions as the numbers of CFU/ml obtained for these two conditions are below the detection threshold of this test.

Killing kinetic of the *ialB* mutant in starvation

Following the previous results, it was decided to experimentally determine whether or not the CFU decrease in PBS is induced rapidly or slowly. Consequently, the mutant was incubated in PBS and plated at different time points. Each experiment had the same first (T_0, in minutes) and final (T_{120}) time point but the intermediate times were variable since a more precise estimation was expected after each experiment. The first experiment suggested a rapid kinetic because no colonies were observed as soon as the initial time point. With the second, colonies were found on every plate except the T120 plate. Finally, the last experiment rather proposes an entirely different outlook since no significant differences were observed between the two strains.

Morphology of the *ialB* mutant

As a 2 hours long PBS incubation seemed to greatly affect the *ialB* disruption mutant, it was observed by phase contrast microscopy in order to see whether or not the morphology has changed. Because, as for the pH, it has been reported that the temperature can have an impact on the *ialB* expression level, mutants incubation were done at room temperature (RT) and 37°C. The images taken by phase contrast microscopy (Fig. 13) show similar phenotypes before the incubation for both strains. However, after 2 hours in PBS, the mutant shows a different phenotype than the WT with a lighter centre that might reflect a swelling of the bacteria.

Membrane integrity of the *ialB* mutant

Following the observation of a possible swelling, it was decided to test the membranes integrity. This was achieved by using propidium iodide, which is employed in a common envelope permeability assay. When the membranes are intact, propidium iodide cannot enter into the bacteria. On the contrary, once the envelope has undergone abundant damages, the bacteria are stained and it is accepted that, at this point, the cell is no longer viable (Davey *et al.*, 1996). In order to have a positive control, the WT strain was preliminary treated with 70% ethanol and that was assumed to disrupt the membranes. Regarding the negative control, it was simply the WT strain, untreated. The data (Fig. 14) show no fluorescence in the disruption mutant; this suggests that its envelope is still impermeable to propidium iodide and therefore, is not heavily damaged.

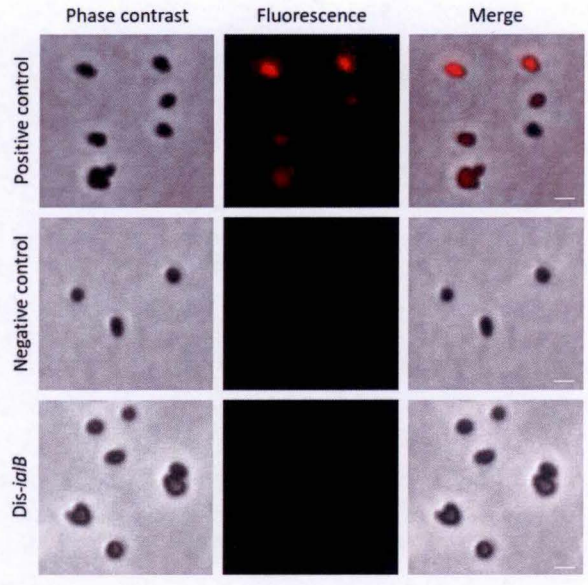

Figure 14 | Dis-*ialB* membranes integrity test. This was performed with propidium iodide (in red) and aims to reveal any membrane damages that would compromise its integrity. The positive control shows the method reliability and represents the WT strain incubated 5 minutes in 70% ethanol while the negative control is the WT strain untreated and shows no labelled bacteria. The results obtained with the disruption strain indicate that the envelope is likely to be intact. Scale Bars represent 1 µm.

Deletion mutants

The aim of a deletion strain is to remove the whole gene by homologous recombination. Contrary to the disruption mutants, there is no remaining part from the gene and no selection pressure is needed to avoid the loss of the mutation (in the previous strains, the addition of kanamycin was necessary). Due to the results obtained with the disruption strains, it was decided to focus on IalB and OppB and let BAB2_0412 aside. Removing one gene part of an operon may be problematic when the encoded proteins form a complex, since the expression of only a part of the complex could be toxic, and generate phenotypes that are not caused by the absence of the gene of interest *per se*. Consequently, the whole operon (Fig. 7) was removed from the genome to avoid any deregulation of the operon genes. As this operon has been identified as homologous to the Opp system, the mutant will be named Δ*opp*. Despite many attempts, no *ialB* deletion mutant could be obtained. The reasons for this are not completely clear and hypotheses are detailed in the *Discussion*. It should be noted that the disruption mutants were all constructed in a *B. abortus* 2308 background but the deletion was also performed in a *B. abortus* 544 strain for reasons that will be developed later.

Wild Type and Δ*opp* strains growth

Following the observation of the small colony phenotype with the *oppB* disruption mutant, it was decided to monitor the strains growth. The aim was to assess whether or not this phenotype was intrinsic (i.e. due to the strain) or was due to specific environmental factors encountered during the infection or the PBS incubation. Due to a failure of the growth-monitoring machine (Bioscreen), growth analysis was performed once and manually by measuring the optical density (OD) of WT and mutant strains (in the 2308 and 544 wild types background) cultures over 50 hours. The results (Fig. 15) show that the two strains (i.e. 2308 and 544) exhibit different profiles and that, in both backgrounds, the mutant strain has a delay compared to the WT. However, the delay does not occur at the same point since for the 2308 strain it begins as soon as the 5 h time point (Fig. 15A), but for the 544 strain it begins at the 10 h time point (Fig. 15B). Regarding the two profile differences, it appears that not only they reach their stationary phase at a different time but also in a different way. Indeed, while the 544 strains have a fast and marked exponential phase the 2308 has a slower growth and it reaches its stationary phase later. Finally, concerning the 2308 strain, its exponential phase seems to be divided into three steps, the first from 0 to 5 h, the second from 5 h to 15 and the last from 15 up to the beginning of the stationary phase.

Morphology of the Δ*opp* mutant

Because the mutant delay observed in the growth monitoring could go with a morphological impairment, it was decided to check the strains phenotype based on bacteria coming from 2YT cultures incubated for 50 hours at 37°C. This late time point was chosen as if a phenotype had to appear at any stage during the growth, it would obviously be noticeable after 50 h in culture. As shown by the phase contrast microscopy images (Fig. 16), no morphological difference was observable between the WT and the mutant strain.

Virulence of the Δ*opp* mutant in RAW 264.7 macrophages

In order to confirm the data obtained with the disruption mutants, 2 h infections of RAW 264.7 macrophages were performed with the deletion as well as the WT strains. The data showed no difference between the WT strains and their associated mutant in term of CFU number (Fig. 17). Also, these data are consistent when compared to those obtained with the disruption mutants as they happen to be in the same range of values (Fig. 8). It should be noted that the data only represent a single experiment. Indeed, in the replicate, the 2308 WT strain

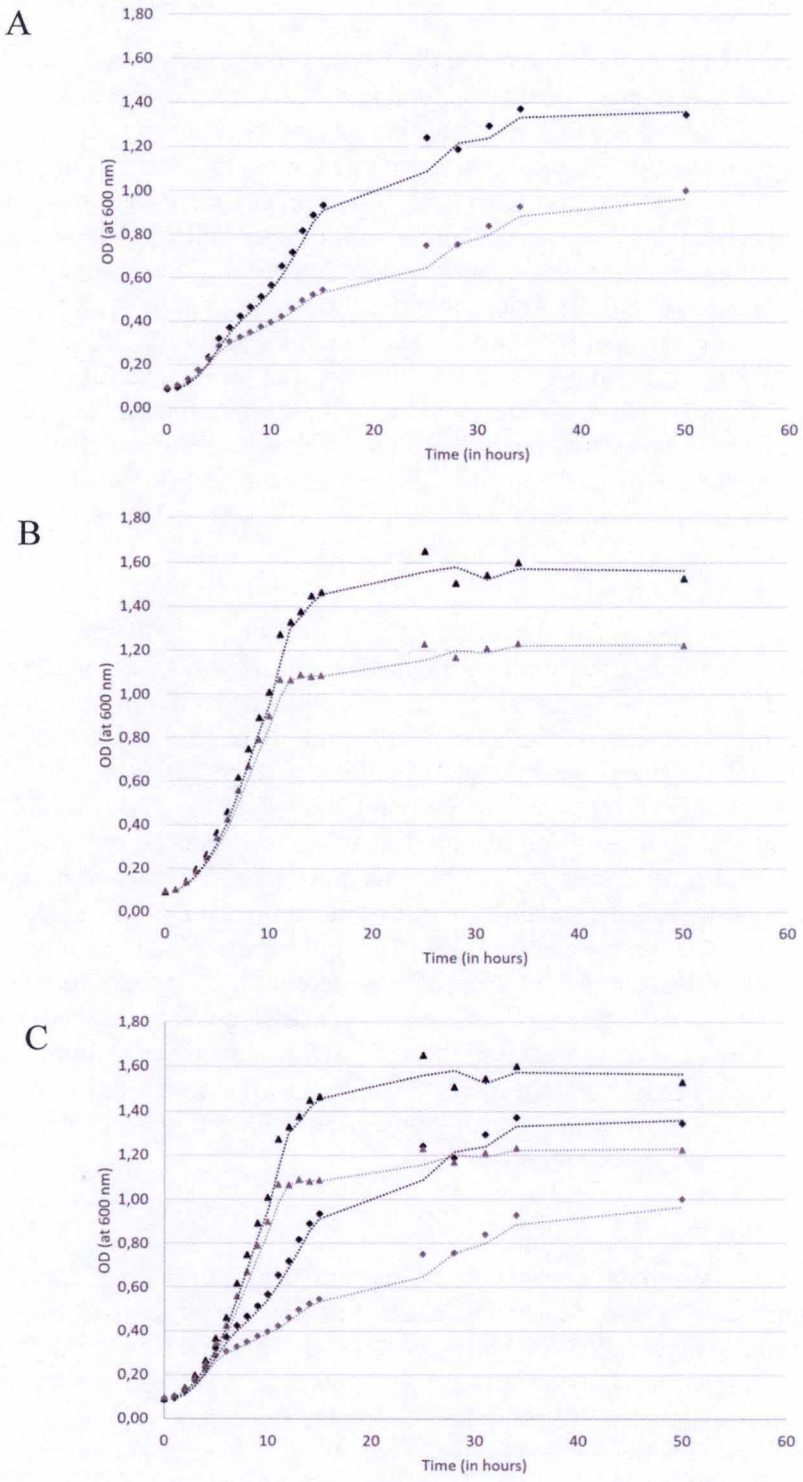

Figure 15 | WT and mutant strains growth curves of *B. abortus* 2308 (A), *B. abortus* 544 (B) and merged graphs (C). Each symbol represents a measure and the total length of the monitoring was 50 hours after the first measurement. The triangles represent the WT strains and the diamonds the mutants. The dotted lines are the tendency curve that are represented to smooth the curve as the manual measurements may cause slight variations. In both backgrounds, the mutants exhibit a growth delay. However, it does not take place at the same time since for the 2308 strain, it seems to begin around 5 hours after the first measurement while for the 544 strain, and it seems to coincide with the very beginning of the stationary phase. Another noticeable difference is the exponential phase appearance since for the 544 strain, there is a characteristic exponential profile and the 2308 phase seems to be slower, biphasic or triphasic, and longer.

showed different colony sizes and growth issues that suggested an abnormal population heterogeneity that is usually not observed. It should be noted that the term *"abnormalities"* associated with the 2308 strain used in the rest of this work refers to this description and will not be developed anymore. Consequently, the CFU numbers would not have been representative. Although the replicate results cannot be used here, the 544 data are shown for information in the *Supplementary data* as they support the 544 strain data shown on Fig. 17. Furthermore, no other replicates were done due to a centrifuge breakdown in the BSL3.

As for the disruptions mutants, 24 h infections were performed. Here again, the 2308 strain had such growth problem as developed above that the counting was not possible and its data could not be taken into account. Expectedly, the results (Fig. 18) show no difference between the 544 Δ*opp* and the WT bacteria. Once again, the 24 h PI CFU number are supported by the data of the disruption mutants (Fig. 9). Again, no replicate could be performed because of the centrifuge breakdown.

B. melitensis Tn-seq data analysis

By the end of this project, another Tn-seq was performed in the URBM by Georges Potemberg. It was different in several aspects compared to the *B. abortus* one described in the *Introduction*, since it focused on *B. melitensis* 16M and the infection model was mice instead of macrophages. Also, the control condition was changed as, after the library construction, bacteria were recovered, pooled and underwent a second round of culture on 2YT plates. Regarding the infection, while a 5 h PI and 24 PI time point were performed, only the 5 h PI data could be compared as the number of reads was not sufficient for the 24 h time point.

The raw data were then treated using Galaxy Project website, an online platform of bioinformatics tools. These data were processed in order to have the same output as the initial Tn-seq. Briefly, the data were mapped onto a reference genome, then the reads were sorted by position onto this genome and finally the number of reads per position was counted. Nevertheless, this last part will not be detailed here since it is not interesting for this work, exception made of the genes studied here. Interestingly, when looking at the obtained results (Fig. 19), *ialB* is indicated as essential as soon as the second plating on rich medium in the control condition. This is very interesting because it could explain why it was impossible for us to generate a deletion strain for *ialB* in *B. abortus*. Even though less striking, a pattern of decreased fitness is observed for the *opp* region. As on Fig. 7C, the BAB2_0700 homologous seems less impacted than the rest of the operon. Unfortunately, the two control conditions cannot be compared as only the data set of the second round of culture was available. Moreover, the *Brucella* strain is different, which further complicates the analysis.

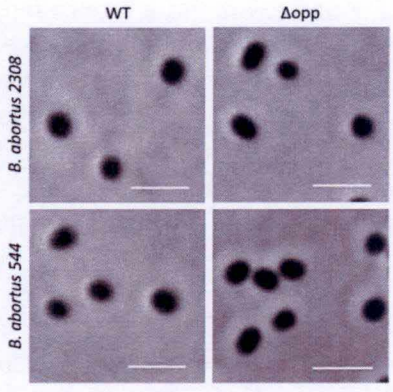

Figure 16 | Phase contrast microscopy of the two WT strains as well as the two mutants Δ*opp* after 50 hours of cultures in 2YT. As depicted on the images, no significant difference can be observed between the WT and the corresponding mutant strain. Scale bars represents 2 µm.

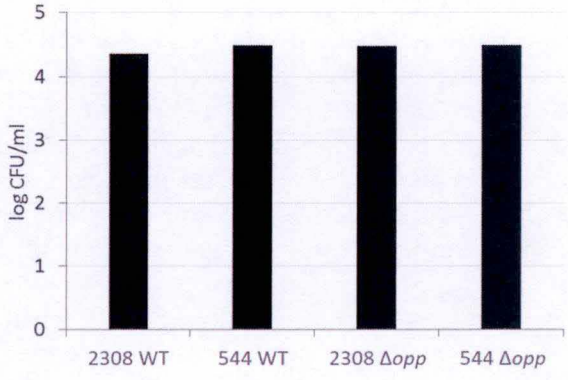

Figure 17 | Number of CFUs (logarithmic scale) for the two WT strains and the two Δ*opp* corresponding mutants after a 2 h infection in RAW 264.7 macrophages. No difference in CFU number can be observed between the different strains here. The deletion mutants' values are similar to those obtained with disruption strains in the same experimental setup. No errors bars are present as the 2308 exhibited different colony sizes and growth issues that suggested an abnormal population heterogeneity that is normally not observed. These abnormalities prevented any statistical analysis and no triplicate was possible for the 544 strain due to a breakdown of a centrifuge in the BSL3. Nevertheless, another graph can be found in the *Supplementary data* (Fig. S1) showing the data for both 544 strains.

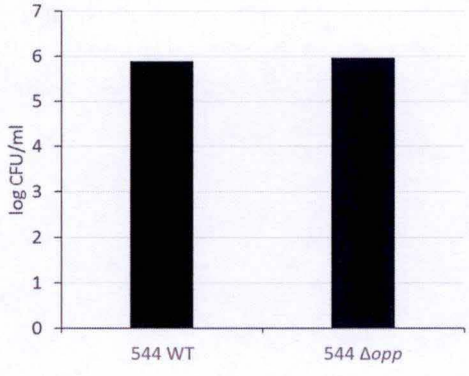

Figure 18 | Number of CFUs (logarithmic scale) for the 544 WT strains and the corresponding Δ*opp* mutant after a 24 h infection in RAW 264.7 macrophages. No difference can be observed between the two 544 strains. Regarding 2308, strong dissimilarities prevented a reliable CFU counting explaining why the 2308 strains are not shown. Nevertheless, these data are consistent with those obtained 24 h PI with the disruption mutants.

Discussion and perspectives

By performing the experiments presented in the *Results*, several unexpected observations stood out. Among them, the most striking is the differences between the predicted fitness by the Tn-seq and the infections results. The abnormalities observed with the 2308 strain were also of concern as it jeopardizes the outcome of some experiments, as explained in the *Results* section. Finally, the data generated by the Tn-seq in *B. melitensis* gave interesting results in the sense that the orthologues of the two studied genes were already identified as necessary for the growth on rich medium. Consequently, this discussion will be divided into two parts: the first one discusses the results in their generality while the second will focus on the Tn-seq technique itself.

IalB

First annotated as an invasion protein, BAB1_0491 was then identified as homologous to *ialB* by using a conserved domain identification tool. While no clear molecular function has been established for IalB, it has been reported as crucial for the human erythrocyte parasitism in *B. bacilliformis* (Coleman and Minnick, 2001). Regarding the disruption mutants, *ialB* had the most promising phenotypes. Indeed, the CFU decrease observed after 2 h of macrophage infection was consistent with the Tn-seq data. Even though a decrease was also observed after 24 h, no statistical difference was found with the WT, probably because of variations between replicates. Following a PBS incubation during 2 h, the *ialB* disruption mutant exhibited the same decrease as in infection when compared to the WT. Because PBS was used to mimic the starvation encountered in the intracellular trafficking, these results indicated that the decrease could be related to nutrient depletion. The morphology was then characterized by phase contrast microscopy before and after the 2 h PBS incubation. Whereas the WT and the disruption strain had the same phenotype before the incubation, the mutant appearance turned out to be different afterwards. Indeed, even if the mutant still had a round shape characteristic of a stationary phase, bacteria seemed bigger, rounder and their centres were lighter. This was thought to likely reflect a swelling of the bacteria and because such morphology could be related to membranes damages, the membranes permeability was tested. The obtained results could not demonstrate any heavy damages and it was therefore assumed that the membranes integrity was maintained.

Considering those interesting observations, it was then decided to engineer a deletion strain. Even if deletion strains were eventually required and are considered as more reliable for investigations, disruption strains were nonetheless important. Indeed, they allowed to have a rapid evaluation of the gene's potential functions, as the limited time was a constraint along this work. Furthermore, the Tn-seq data were generated by transpositional insertions and therefore, gene disruptions.

However, after several deletion attempts and hundreds of clones tested, no deletion could be achieved. Inevitably, this failure raises the question of why the disruption was manageable but not the deletion. If there is no clear reason for that, hypotheses can be emitted and the most likely is that the gene is already essential for growth under the conditions used here. Nevertheless, because the disruption was possible, a fragment of the encoded protein might be sufficient to ensure, at least partially, the function, or to allow the quick generation of suppressors. Consequently, it is important to understand why the Tn-seq data predicted that *ialB* is important during the infection only. Elements of response are brought and discussed in the Tn-seq related part of the discussion.

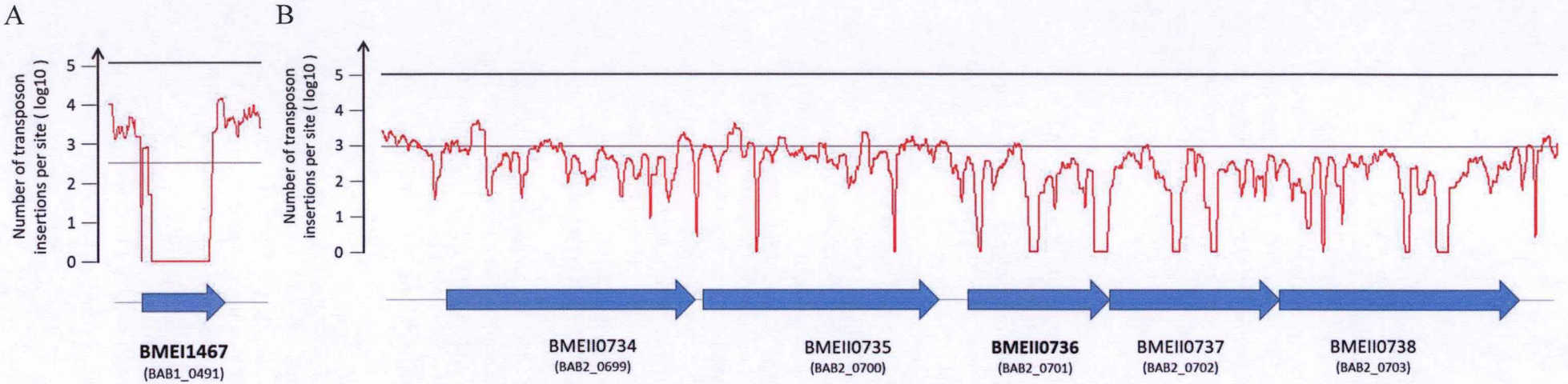

Figure 19 | Number of transposon insertions per site (log 10) for *ialB* and *opp* operon homologues in *B. melitensis* for the control condition. Both graphs represent the gene fitness in control condition after the second round of culture in *B. melitensis*. The Y axis indicates the number of transposon insertions per site that are shown by the red line on the graph and the X axis represents the genome map. The graph possess two straight lines; the light grey is the chromosomal mean transposon insertion number and the dark grey represents the maximum insertion number observed. If the essentiality is clearly marked for the *ialB* homologue gene (BMEI1467 in *B. melitensis*), it is not the case for the *opp* operon. However, this is explained by the fact that the R200 has not been calculated for this data set. Nevertheless, the curve being most of the time under the average number of insertion per site line is an indicator of a decreased fitness for this region.

oppB *and the* opp *operon*

Contrary to the *ialB* mutant, the disruption of *oppB* did not produce any CFU decrease in infection compared to the WT, neither at 2 h PI nor at the 24 h PI time points. However, it was noticed that the *oppB* disruptant formed smaller colonies than the other strains after a macrophage infection. Consequently, small colonies were isolated and were able to restore a WT phenotype after a second round of culture. Interestingly, those observations suggested that the growth delay was likely to be caused by the infection process. As all disruption strains were grown on kanamycin supplemented media, it was then proved that the antibiotic was not responsible for the growth delay. It should be noted that possible combined effects of the infection and the kanamycin have not been ruled out.

Even though no CFU attenuation was observed, the slower growth after the infection was intriguing. Consequently, the deletion was performed but, rather than removing only *oppB*, the whole operon was deleted. Indeed, the suppression of one gene part of an operon might be problematic for two reasons. First, as developed above, the expression of only a part of the complex might generate a toxicity. Secondly, the deletion might reduce the distance between the operon promoter and the genes downward. The latter might then be upregulated and cause toxicity. Because it had been noticed that the 2308 strain had growth defects, the *opp* operon has also been engineered in a *B. abortus* 544 background. This strain was chosen as it has been extensively used in the laboratory and its genome is sequenced. Finally, it should be noted that at the same time, another stock of 2308 was used for the *opp* deletion because the end of the usual stock had been reached.

Because the small colonies observed after the infection were probably due to a slower growth, it was decided to monitor the strain growth over 50 hours. In both backgrounds, the mutant exhibited a growth delay compared to the WT. Noticeably, the delay seemed to have the same amplitude in both cases but, it did not take place at the same time. Indeed, the delay began around the 5 h time point for the 2308 deletant which coincides with the exponential phase beginning. For the 544 mutant, it started later as it becomes noticeable at 10 h which seems to be the beginning of the stationary phase. Due to a failure of the Bioscreen, those curves were obtained manually and replicates will have to be performed with the appropriate equipment. Nevertheless, the 544 values were compared with pre-existing data and both data sets matched, supporting those results. In the future, growth curves should also be performed for a complemented mutant as the complementation vector has been designed in the course of this master thesis.

As the *oppB* is predicted as part of an oligopeptide transporter, a role in the nutrient acquisition seems to be the most likely hypothesis to explain the slower growth of the mutant strain. Furthermore, it is proposed that the *Brucellae* would not produce any extracellular hydrolytic enzymes acting on proteins, nucleic acids, and polysaccharides (Moreno and Moriyón, 2006). Consequently, *Brucellae* would solely rely on low molecular weight nutrients already present in the environment, like amino acids and small peptides. While speculative, it is possible that Opp allows the bacterium to use a specific source of nutrients like small peptides, which are abundant in the rich medium. Therefore, if Opp is deleted, the mutant might have a nutrients uptake defect that could explain the growth delay with the WT. So as to test this hypothesis, it would be interesting to assess different sources of nutrients to determine which one could be responsible for the phenotype. As a control, it would be interesting to cultivate the mutant in a defined medium like the Plommet medium, with erythritol as the sole carbon source.

In *E. coli* and *S. typhimurium*, the oligopeptide transporter has been identified to solely mediate the uptake of cell wall peptides (Goodell *et al.*, 1987). Also, it has been shown that in one generation time, *E. coli* is able to renew up to 50 % of its peptidoglycan (PG) (Goodell, 1985). Even though murein represents a substantially smaller part of the Gram-negative cell mass compared to the Gram-positive bacteria, recycling the PG peptides could help to deal with a sudden nutrient depletion stress. Indeed, it has been shown that cell wall peptides are reincorporated in murein and its precursors only (Goodell *et al.*, 1987). Such a stress being similar to what *Brucella* can encounter during the macrophage trafficking, this could explain why this transporter has been identified as important during the infection. Supporting the Tn-seq data, it has also been reported that the recycling pathway is not essential for the growth under laboratory conditions (Boudreau *et al.*, 2012). Interestingly, the two major cell wall peptides contain D-amino acids and have a γ-peptide bond. The uptake of peptides with such characteristics has been predicted to be less efficient compared to protein-derived peptides which usually contain L-aa and possess an α bond (Goodell *et al.*, 1987). However, because their import has been demonstrated, the cell wall peptides could be an exception as their sequences are well defined because of their small diversity. Also, following substrate-binding competition experiments, it has been proposed that OppA, the periplasmic component of the transporter whose function is to bring substrates to the permease, could possess more than one peptide-binding site with overlapping functions that would explain its broad action spectrum (Guyer *et al.*, 1985). Nevertheless, the differences between the two OppA homologs present in this *Brucella* remain unknown as well as why only one out of the two has been identified as important during the infection. Based on the large variety of substrates in this family of proteins, one hypothesis is that it could be due to a different substrate specificity between the two OppA homologues. Consequently, further experiments would be necessary to confirm their respective specificities.

In *C. difficile*, it has been demonstrated that Opp, through the peptides import, normally inhibit the sporulation. When the stationary phase is reached, peptides import is decreased, and thus the repression of sporulation is impaired, allowing the bacteria to sporulate at this culture phase (Edwards *et al.*, 2014). Although *Brucella* does not sporulate, a possible role of Opp in signaling the growth state should be considered. Without the transporter, it is possible that the bacterium has a signalling leading to a growth impairment, by an unknown mechanism. While the most likely Opp explanation is related to the nutrients uptake, no lead should be neglected.

From an immunological point of view, it should be noted that the muropeptides are considered as pathogen-associated molecular patterns (known as PAMPs). PAMPs are recognized by the NLRs (Nod-like receptors), that are part of the pattern recognition receptors (PRRs), and more especially by NOD1 and NOD2 (Boudreau *et al.*, 2012). Because an immune response against the bacterium could be triggered if there is a ligand-receptor recognition, any muropeptide leak has to be avoided. Consequently, the cell wall peptides recycling pathway is even more important in an infection context. To assess the hypothesis of a more intense release of muropeptides in the mutant strain compared to the wild-type control, the concentration of cell wall peptides could be following incubation in a defined medium, such as Plommet, where the bacteria can grow but no peptides are present.

The last point regarding the *opp* operon concerns its genetic environment. Right after the ABC transporter genes is located the *alkB* gene. The encoded protein is induced to reverse the DNA alkylation damages. However, Katy Poncin (from Xavier de Bolle's team) has observed that while a Δ*alkB* mutant is viable, the complementation with a WT allele of *alkB* is complicated. Indeed, as soon as there is an overexpression of *alkB* (even small), the strain

experiences growth defects and reaches its plateau at an OD of about 0.6 (Katy Poncin, personal communication). Removing the whole operon could cause a deregulation of *alkB* expression, probably an overexpression, and explain the growth delay of the Δ*opp* strain compared to the WT strain. One way to test this hypothesis would be to test the *alkB* deletion in the Δ*opp* background, expecting to remove the growth delay observed with the Δ*opp* strain by deleting the potentially toxic *alkB* gene. As shown by the Tn-seq profile of the *opp* operon, the second *oppA* homologue has not been identified as important. This means that, if the transposon insertion had caused a deregulation of *alkB*, all the genes should appear as important. It is, therefore, unlikely that *alkB* overexpression is responsible for the attenuation of the *opp* mutants in the Tn-seq experiment.

B. abortus 2308 strain

As reported in the results, abnormalities have been noticed regarding the 2308 WT growth during the experiments. Indeed, several infections data could not be used here due to abnormal growth and highly variable CFU numbers from one experiment to the other. These observations were later supported by growth monitoring that showed an abnormal exponential phase and a stationary phase happening too early. The 2308 strain being used as the reference strain in the United States, those observations may challenge the notion of reference strain in this work context. This idea is not solely based on this work: in September of this year, a paper analyzing three *B. abortus* 2308 genomes from three different laboratories found out that they showed significant differences. Indeed, they first identified three major deletions (of 1.13, 3.4 and 5.7 kb) between their strains, then an insertion of 5.2 kb was found as well as an inversion of the genomic island 5 of 47 kb. Also of notice, insertions elements were found to surround these genome modifications (Suarez-Esquivel *et al.*, 2016). Another example supporting this idea comes from findings made in 2012 by Mancilla and co-workers. The researchers found, that due to spontaneous excision of a gene related to the O-chain biosynthesis of the LPS, the bacterium switch from smooth to rough lipopolysaccharide. As in the previous study, the many insertions sequences found in *Brucella* genome are thought to play a role in this excision. Indeed, they are believed to favor the homologous recombination leading to the deletion. (Mancilla *et al.*, 2012).

In this respect, these findings exemplify how unstable *Brucella* genome is and how genetic diversity can emerge. This also demonstrates that the term "*reference strain*" should be used with caution as it is not as straightforward as it might seem. Regarding this work, it is hard to identify what caused the 2308 abnormalities. One reason could be related to its storage conditions, even though considered as the current standard, the defreezing and refreezing cycles might change in some way the nature of the bacteria. Another reason could be related to the genome instability and, to highlight such variability, one could sequence the strain genome and compared it to the publicly available genome to have a new outlook on the situation. If the project had to be continued, 544 would probably be recommended as a reference strain, it has been well characterized in this laboratory.

The Tn-seq

As this work is based on the data generated by the Tn-seq on *B. abortus* mutants and their fitness in RAW 264.7 macrophages infection, the technique possibilities and limitations should be discussed. Even though the genus *Brucellae* is considered as genetically homogenous, repeating the experiment with different species might be relevant as species-dependent features might exist. Also, as discussed above, even two *a priori* similar strains (2308 and 544 for example) might exhibit genomic particularities that could bias the technique.

Indeed, if a gene has been excised, it will appear as essential in the Tn-seq profile. There is also many possibilities regarding the infection models with, on the one hand, the cellular models, and on the other hand, the living models. For the latter, the best models would obviously be the natural host but due to the *Brucella* manipulation constraints, this would require onerous facilities. Concerning the cellular models, many cell types are available to perform infections. Their relevance will depend on the characterization of the intracellular *Brucella* trafficking and on the bacteria replication. Consequently, many combinations are possible and choices should be made by taking in account the model relevance.

Regarding the limitations, two mains factors might affect the generated data. First, even if a gene is essential or important but redundant, no effect will be seen. This is because, theoretically, there is only transposon insertion per genome for each mutant. The other factor is related to the strain growth. Indeed, if a strain grows slower, less identical genotypes will be found compared with a normally growing strain after same amount of time. Because the Tn-seq data are based on a number of transposon insertions per site, a slower growth could, therefore, appears as a reduced fitness. This could explain the observed phenotype for *oppB*. Unfortunately, these effects are inherent to the technique and cannot be avoided.

In the meantime this project took place, two other Tn-seq were performed within the laboratory. The first was conducted with the same 2308 strain on trophoblasts while the second aimed to highlight *B. melitensis* important genes in a mice infection model. Although in trophoblasts, the results reported were consistent with the data generated in RAW 264.7 macrophages; the second Tn-seq revealed unexpected results for the orthologous genes studied here. In the control condition (library plated two times), *opp* is already indicated as important for growth and *ialB* is now essential.

Before developing these contradictory results, it should be reminded that the cause of these dissimilarities could simply be related to the species difference. Perhaps *ialB* is not present in the *B. melitensis* 16M strain used in the Tn-seq and that would explain is essentiality pattern. It could also be related to the differences between the two control conditions. Indeed, for the *B. melitensis* Tn-seq control, the mutants underwent a second round of culture after they have been pooled. Consequently, it is possible that this second round intensifies a growth defect that would appear as a fitness decrease. Also, it is possible that in the absence of the second round of culture, gDNA from dead bacteria is retrieved. Although it is not known whether or not gDNA is degraded, this could bias the data by not predicting the importance of a gene. To solve these issues, the first step would be to sequence the genome of the *B. melitensis* 16M strain used for the Tn-seq allowing to precisely know what genes are present or missing, and where they are. Secondly, it is crucial to investigate the effect of a second plating on the data. In this respect, another Tn-seq has been performed with *B. abortus* in the frame of this master thesis, but the analysis is still ongoing and sequencing data could not be received in time for this work.

Conclusion

In conclusion, as this work has come to an end, it raised many questions on different topics. Despite the lack of clear data for *ialB*, understanding its precise role within *Brucella* might still be of interest. Even though it does not seem to play a role in the infectious ability, its importance in culture is suggested by its apparent essentiality. Regarding Opp, while no precise phenotype could be highlighted, its broad potential of functions reflects the complexity of its study. However, this versatility could also be promising and further investigations should be performed in order to assess the potential of the different hypothesis developed above. Eventually, this could lead to the understanding of this transporter importance during the macrophage infection. Finally, the ongoing Tn-seq will certainly bring new elements of response regarding the importance of appropriate controls for this new technology.

Concerned gene	Name	Sequence
BAB1_0491	1-0491_disrpt_F	5' – AGA CAC CGG CGG AAC CAC AG – 3'
	1-0491_disrpt_R	5' – AAG ATC GTC TTC CAG AAT GAC TTC – 3'
	491 dis check	5' – CTG GAA GAC GAT GAA GG – 3'
	491_del_AM_F	5' – GTT GCG GCA ACA ATC TTA TCC A – 3'
	491_del_AM_R	5' – GGA ATG TGA CGT GCG GTG GGC AAA CA – 3'
	491_del_AV_F	5' – CAC CGC ACG TCA CAT TCC CGC AGA CTG AG – 3'
	491_del_AV_R	5' – TAG GCG TCG ATC TGT TGC AGA A – 3'
	491_check_del_F	5' – TCC ACA GCA CTG CCA GAG – 3'
	491_check_del_R	5' – CAT GCA AGC GAA ACA GAT ACT TG – 3'
BAB2_0412	2-0412_dirspt_F	5' – CAT ATT GGG TTC GCT GAT CG – 3'
	2-0412_dirspt_R	5' – CAC ATG CAG GAG ATA GAT GAG – 3'
	412 dis check	5' – TTT CTC ATC ACG CCA CT – 3'
BAB2_0701	3-0701_dirspt_F	5' – GAT CAT ACT CGG CACA GCT TG – 3'
	3-0701_dirspt_R	5' – CGA AGT GCC TCG ATG GTT G – 3'
	701 dis check	5' – ACT TCA CGG TGA ACG AT – 3'
	Opp_del_AM_F	5' – AGG CTT GAT CGG CTC ACA – 3'
	Opp_del_AM_R	5' – TCA TCC ATT CGA AGA ACC CCT CCG TTG A – 3'
	Opp_del_AV_F	5' – GTT CTT CGA ATG GAT GAA TAA GCG CTT C – 3'
	Opp_del_AV_R	5' – AGT GAA ACG GAA ACG ATG GGA T – 3'
	Opp_check_del_F	5' – CCT TAT TGT GGG CGT TCT G – 3'
	Opp_check_del_R	5' – GGT GCA GGA TAT ATT TGG TGA TC – 3'

Table 2 | Table of primers.

Material & methods

Strains

All *Brucella* strains used for the experiments described in this work were grown in 2YT rich medium (1 % yeast extract, 1.6 % peptone, 0.5 % NaCl). *E. coli* strains were cultured in Luria-Bertani broth medium. Following antibiotics concentrations were used: ampicillin (100 µg/ml), chloramphenicol (20 µg/ml), kanamycin (10 µg/ml for chromosome-encoded resistance or 50 µg/ml for plasmid-borne resistance) and nalidixic acid (25 µg/ml).

Disruption strains constructions

For disruption mutants, a homologous region from the gene to be disrupted of about 300 base pairs was amplified by PCR and inserted into the plasmid (see *Restriction* and *Ligation*). The recombinant plasmid was then transformed into a donor *E. coli* strain (see Transformation) to be transferred in *Brucella* (see Conjugation) and could, therefore, integrate *B. abortus* genome through homologous recombination, conferring to the strain kanamycin resistance and sucrose sensitivity. Plasmid used for the strains construction was pNPTS138, encoding a kanamycin resistance cassette (*npt1*) and a sucrose sensitivity gene (*sacB*). Primers used during this process are detailed in Table 2.

Deletion strains constructions

For the deletion mutants, two regions (one upwards and one downwards the gene) of 500 base pairs were amplified by PCR. Then, these two fragments were fused together *via* a small region of complementarity designed in the primers. Once this 1000 base pairs fragment amplified, it was inserted in a pNPTS138 plasmid this construction was cloned (see *Transformation* and *Plasmidic DNA extraction*) in a DH10B *E. coli* strain and purified. The plasmid was then inserted in a donor S17 *E. Coli* strain to perform an integrative plasmid conjugation (see *Conjugation*). Following this, 3 colonies were streaked and once the streak fully grown, one was cultured overnight in 2YT without any antibiotic. 100 µl of this ON culture were spread on 5% sucrose 2YT-agar. Then, 100 of the grown clones were streaked in parallel on kanamycin (10 µg/ml) 2YT-agar and 5% sucrose 2YT-agar. This step allowed to discriminate the bacteria that still had the plasmid integrated from those who lost it. After that, deletion strains were discriminated from the WT strains by diagnostic PCR.

Plasmidic DNA extraction

1 ml of an overnight culture of *E. coli* DH10B carrying the adequate plasmid was centrifuged at 13,000 RPM for 1 minute and supernatant was discarded. To increase the bacterial pellet, this was done twice. Then 300 µl of P1 buffer (RNase A 100 µg/ml, TrisHCl 50 mM, EDTA 10 mM, pH 8) at 4°C was added and used to resuspend the bacteria. Next, 300 µl of P2 buffer (NaOH 200 mM and 1 % SDS) were added and the suspension was mixed by inversion 5 times and was incubated 5 minutes at RT. The following step consisted in adding 300 µl of P3 buffer (potassium acetate 3M). Centrifugation at 13,000 RPM for 10 minutes was performed and the supernatant was retrieved. 700 µl of isopropanol were added and the resulting solution was thoroughly mixed. After a centrifugation of 10 minutes at 13,000 RPM, the supernatant was discarded and 400 µl of ethanol were added on the side of the pellet. The tube was then

centrifuged at 13,000 RPM for 5 minutes and the supernatant was once again discarded. The pellet was dried in an incubator at 55°C. Once dry, 20 µl of water were used to resuspend the pellet.

Genomic DNA extraction

After *Brucella* inactivation (1h at 80°C), cells were centrifuged at 13,000 RPM for 1 minute. The supernatant was then discarded and the pellet was resuspended with 567 µl of TENa (Tris pH 8 50mM, EDTA 50 mM and NaCl 100mM), 30 µl of 10 % SDS, and 3 µl of Proteinase K (20 mg / ml). The pellet was resuspended and the mix was incubated and agitated at 37°C overnight. The cloudy mixture should then become translucent. Then, the protocol is the same as the plasmidic DNA extraction protocol, beginning at the isopropanol step.

PCR

Each preparative PCR mix contained Q5 high-fidelity DNA polymerase (100X, 2,000 U/ml, BioLabs), Q5 reaction buffer (5X, BioLabs), dNTPs (2.5 mM each, Takara), template DNA, milliQ H_2O (milliQ purification system, Millipore) and forward and reverse primers (20 µM each) for a final volume of 50 µl. The PCR steps were the following; first, a denaturation step at 98°C during 30 seconds and next, 30 amplification cycles. A cycle included a DNA denaturation step (10 seconds a 98°C), a primer hybridization step (temperature was adapted according to the primers sequences during 30 seconds) and an elongation step at 72°C (the amplification step time was set according to the PCR product length, considering a speed of 2000 nucleotides per minute). The last step was a final elongation at 72°C during 5 minutes.

Purification of PCR products

Purification was achieved by using the NucleoSpin, Gel and PCR Clean-up kit (Macherey-Nagel) according to manufacturer instructions.

Enzymatic restriction

DNA restriction was performed with the appropriate restriction enzyme (10X, Roche) and buffer (10X, 5 U/µl, Roche) during 40 minutes at 42°C. DNA quantity vary depending on the type; about 300 ng for preparative restriction and about 120 ng for diagnostic restriction.

Ligation

The ligation of inserts into plasmid was achieved by mixing the ligase enzyme (10X, Invitrogen), the appropriate buffer (5X, Invitrogen), 5X restricted plasmid and the insert 5X. The mix was then incubated overnight at RT.

Transformation

Transformation was performed using the competent *E. coli* strain DH10B. Once thawed, 3 minutes on ice (4°C), ligation mix was added at a concentration of about 300 ng/ml. Bacteria were then incubated on ice for 20 minutes and a heat shock at 42°C during 2 minutes was then performed. For the recovery, 700 µl of LB medium were added and the bacteria were then placed at 37°C and shaken for 45 minutes. Once the incubation time was over, tubes were centrifuged at 5000 RPM for 3 minutes. Supernatant was partially removed to leave approximately 100 µl. Finally, the pellet was resuspended and plated on LB-agar medium

containing the appropriate antibiotic, X-gal (0.004 %) and IPTG (1 mM) in order to perform a blue screen. The petri dishes were incubated overnight at 37°C.

Conjugation

To perform the conjugation, overnight cultures of *B. abortus* 2308 and the conjugative *E. coli* S17-1 carrying the appropriate plasmid were grown. 50 µl of *E. coli* culture was added to 1 ml of *B. abortus* culture. The mix was then centrifuged 2 minutes at 7,000 RPM. Supernatant was removed and 100 µl of 2YT medium were used to resuspend the pellet. Then, the resulting suspension was centrifuged again for 2 minutes at 7,000 RPM. This time, supernatant was partially removed to have 100 µl left, the pellet was resuspended and spotted on 2YT-agar.

For an integrative plasmid, such as pNPTS, half of the drop was recovered the next day and resuspended in 400 µl of 2YT. 100 µl of the bacteria mix was spread on 2YT-agar supplemented with nalidixic acid (1 µg/ml) and kanamycin (10 µg/ml) and incubated for 3 to 5 days at 37°C. The colonies were then streaked on 2YT-agar without nalidixic acid.

RAW264.7 macrophages culture and infection

RAW264.7 macrophages were cultured at 37°C in a 5 % CO_2 atmosphere in DMEM (Gibco) supplemented with 10 % of foetal bovine serum (Gibco). The day before infection, cells were diluted to a concentration of $1.0x10^5$ macrophages/ml. For infections, overnight cultures of the appropriate *Brucella* strains were diluted in RAW culture medium at a multiplicity of infection of 50 (meaning statistically 50 bacteria per macrophage). The RAW medium was removed and replaced by the appropriate bacterial suspensions. The plates were then centrifuged 10 minutes at 1,000 RPM at 4°C. After one hour of incubation, DMEM with gentamycin (50 µg/ml) was added to kill extracellular bacteria, then cells were incubated for the remaining time (2 or 23 hours) at 37°C with a 5 % CO_2 atmosphere.

Normalization of culture

1 ml of an overnight culture were centrifuged at 7,000 RPM for 2 minutes. Once the supernatant discarded, the bacterial pellet was resuspended in 1 ml of PBS or 2YT. Then, the optical density (OD) was measured. For the sensitivity tests, the normalisation was done based on the smallest OD.

Membrane permeability assay

Bacteria were incubated with propidium iodide (1 µg/ml) during 15 minutes in the dark at room temperature. Next, bacteria were washed with PBS. The positive control was performed by incubating the WT strain in 70 % ethanol during 5 minutes then stained according to the method described above.

Microscopy

Brucella strains were observed with a Nikon 80i (objective phase contrast x100, plan Apo) connected to Hamamatsu ORCA-ER camera. For the phase contrast observation of bacteria, 2 µl of culture were laid down on agarose pad (solution of 1 % of agarose in PBS) and sealed with VALAP (1/3 of Vaseline, 1/3 of lanoline and 1/3 of paraffin wax).

Growth measurement

The day before, 4 ON cultures of 10 ml were prepared per strain. The day of the experiment, the 4 cultures were pooled and the OD was measured in order to prepare 100 ml of culture at OD = 0.1 per condition. Then during the 15 first hours, the OD was measured every hours. The measurements for the first day were then stopped and those for the second began 10 hours later (i.e. 25 h after the first measurement) and was done every 3 hours until the 34 h time point was reached. For the last day, two measurements were taken, one a 48 h after the beginning of the experiment and the last one at 50 hours.

References

Al Dahouk S., Scholz H. C., Tomaso H., Bahn P., Göllner C., Karges W., Appel B., Hensel A., Neubauer H. and Nöckler K. *"Differential Phenotyping of* Brucella *Species Using a Newly Developed Semi-automated Metabolic System."* BMC Microbiology BMC Microbiol 10:1 (2010): pp. 269.

Alexander B., Schnurrenberger P. R. and Brown R. R. *"Numbers of* Brucella abortus *in the placenta, umbilicus and fetal fluid of two naturally infected cows."* Veterinary Record 108:23 (1981).

Anderson T. D. and Cheville N. F. *"Ultrastructural Morphometric Analysis of* Brucella abortus-*Infected Trophoblasts in Experimental Placentitis."* The American Journal of Pathology 124:2 (1986): pp. 226-237.

Arellano-Reynoso B., Lapaque N., Salcedo S., Briones G., Ciocchini A. E., Ugalde R., Moreno E., Moriyon I. and Gorvel J.-P. *"Cyclic β-1,2-glucan is a* Brucella *virulence factor required for intracellular survival."* Nature Immunology 6:6 (2005): pp. 618-625.

Arenas G. N., Staskevich A. S., Aballay A. and Mayorga L. S. *"Intracellular Trafficking of* Brucella abortus *in J774 Macrophages."* Infection and Immunity 68:7 (2000): pp. 4255-4263.

Ariza J. Corredoira J. Pallares R., Viladrich P. F., Rufi G., Pujol M. and Gudiol F. *"Characteristics of and Risk Factors for Relapse of Brucellosis in Humans."*Clinical Infectious Diseases 20:5 (1995): pp. 1241-1249.

Atluri V. L., Xavier M. N., de Jong M. F., den Hartigh A. B. and Tsolis R. M. *"Interaction of the Human Pathogenic* Brucella *Species with Their Hosts."* Annual Review of Microbiology 65:1 (2011): 523-541.

Barquist L., Boinett C. J. and Cain A. K. *"Approaches to querying bacterial genomes with transposon-insertion sequencing."* RNA Biology 10:7 (2013): pp. 1161-1169.

Biemans-Oldehinkel E., Doeven M. K. and Poolman B. *"ABC transporter architecture and regulatory roles of accessory domains."* FEBS Letters 580:4 (2006): pp. 1023-1035.

Borezee E., Pellegrini E. and Berche P. *"OppA of* Listeria monocytogenes, *an Oligopeptide-Binding Protein Required for Bacterial Growth at Low Temperature and Involved in Intracellular Survival."* Infection and Immunity 68:12 (2000): pp. 7069-7077.

Boschiroli M-L., Foulogne V. and O'Callaghan D. *"Brucellosis: a worldwide zoonosis."* Current Opinion in Microbiology 4:1 (2001): pp. 58-64.

Boudreau M. A., Fisher J. F. and Mobashery S. *"Messenger Functions of the Bacterial Cell Wall-derived Muropeptides."* Biochemistry 51:14 (2012): pp. 2974-2990.

Bruce, D. *"Note on the discovery of a microorganism in Malta fever."* The Practitioner 39 (1887): pp. 161-170

Celli J., de Chastellier C., Franchini D-M., Pizarro-Cerda J., Moreno E. and Gorvel J.-P. "Brucella *Evades Macrophages Killing via VirB-dependant Sustained Interactions with the Endoplasmic Reticulum.*" The journal of Experimental Medicine 198:4 (2003): pp. 545-556.

Celli J., Salcedo S. P. and Gorvel J.-P. "Brucella *coopts the small GTPase Sar1 for intracellular replication.*" PNAS 102:5 (2005): pp. 1673-1678.

Coleman S. A. and Minnick M. F. *"Differential expression of the invasion-associated locus B (ialB) gene of* Bartonella bacilliformis *in response to environmental cues."* Microbial Pathogenesis 34:4 (2003): pp. 179-186.

Coleman S. A. and Minnick M. F. *"Establishing a Direct Role for the* Bartonella bacilliformis *Invasion-Associated Locus B (IalB) Protein in Human Erythrocyte Parasitism."* Infection and Immunity 69:7 (2001): pp. 4373-4381.

D'anastasio R., Zipfel B., Moggi-Cecchi J., Stanyon R. and Capasso L. *"Possible Brucellosis in an Early Hominin Skeleton from Sterkfontein, South Africa."* PLoS ONE 4:7 (2009)
Davey H. M. and Hexley P. *"Red but not dead? Membranes of stressed* Saccharomyces cerevisiae *are permeable to propidium iodide."* Environmental Biology 13:1 (2011): pp. 163-171.

Dawson R. J. P. and Locher K. P. *"Structure of a bacterial multidrug ABC transpoerter."* Nature 443:7108 (2006): pp. 180-185.

de Figueiredo P., Ficht T. A., Rice-Ficht A., Rossetti C. A. and Adams L. G. *"Pathogenesis and Immunobiology of Brucellosis Review of* Brucella*-Host Interactions."* American Journal of Pathology 185:6 (2015): pp. 1505-1517.

De Lorenzo V., Herrero M., Sanchez J. M. and Timmis K. N. *"Mini-transposons in microbial ecology and environmental biotechnology."* FEMS Microbiology Ecology 27:3 (1998): pp. 211-224.

Deghelt M., Mullier C., Sternon J.-F., Francis N., Laloux G., Dotreppe D., Van der Henst C., Jacobs-Wagner C., Letesson J.-J. and De Bolle X. *"G1-arrested newborn cells are the predominant infectious form of the pathogen* Brucella abortus*."* Nature Communications 5 (2014): pp. 4366.

Dermine J.-F., Duclos S., Garin J., St-Louis F., Rea S., Parton R. G. and Desjardins M. *"Flotillin-1-enriched Lipid Raft Domains Accumulate on Maturing Phagosomes"* Journal of Biological Chemistry 276:21 (2001): pp. 18507-18512

Detilleux P. G., Deyoe B. L. and Cheville N. F. *"Entry and Intracellular Localization of* Brucella *spp. In Vero Cells: Fluoresence and Electron Microscopy."* Veterinary Pathology 27:5 (1990): pp. 317-328.

Edwards A. N., Nawrocki K. L. and McBride S. M. *"Conserved Oligopeptide Permeases Modulate Sporulation Initiation in* Clostridium difficile*."* Infection and Immunity 82:10 (2014): pp. 4276-4291.

Eisenberg T., Hamann H-P., Kaim U., Schlez K., Seeger H., Schauerte N., Melzer F., Tomaso H., Scholz H. C., Koylass M. S., Whatmore A. M. and Zschöck M. *"Isolation of Potentially Novel* Brucella *spp. from Frogs."* Applied and Environmental Microbiology 78:10 (2012): pp. 3753-3755.

Ettema T. J. G. and Andersson S. G. E. *"The α-proteobacteria: The Darwin Finches of the Bacterial World."* Biology Letters 5:3 (2009): pp. 429-32.

Fischer D., Lorenz N., Heuser W., Kämpfer P., Scholz H. C. and Lierz M. *"Absecesses Associated with* Brucella inopinata*-like Bacterium in a Big-Eyed Tree Frog (*Leptopelis vermiculates)." Journal of Zoo and Wildlife Medicine 43:3 (2012): pp. 625-628.

Galinska E. M. and Zagorski J. *"Brucellosis in humans – etiology, diagnostics, clinical forms."* Annals of Agricultural and Environmental Medicine 20:2 (2013): pp. 233-238.

Gatfield J. and Pieters J. *"Essential Role for Cholesterol in Entry of Mycobacteria into Macrophages."* Science 288:5471 (2000): pp. 1647-1650.

Goodell E. W. *"Recycling of Murein by* Escherichia coli*."* Journal of Bacteriology 163:1 (1985): pp. 305-310.

Goodell E. W. and Higgins C. F. *"Uptake of Cell Wall Peptides by* Salmonella typhimurium *and* Escherichia coli*."* Journal of Bacteriology 169:8 (1987): pp. 3861-3865.

Goodwin Z. I. and Pascual D. W. *"Brucellosis vaccines for livestock."* Veterinary Immunology and Immunopathology (2016).

Grégoire F., Mousset B., Hanrez D., Michaux C., Walravens K. and Linden A. *"A serological and bacteriological survey of brucellosis in wild boar (*Sus scrofa*) in Belgium."* BMC veterinary research 8 (2012): pp. 80.

Guyer C. A., Morgan D. G. and Staros J. V. *"Binding Specificity of the Periplasmic Oligopeptide-Binding Protein from* Escherichia coli*."* Journal of Bacteriology 168:2 (1986): pp. 775-779.

Halling S. M., Peterson-Burch B. D., Bricker B. J., Zuerner R. L., Qing Z., Li L-L., Kapur V., Alt D. P. and Olsen S. C. *"Completion of the Genome Sequencing of* Brucella abortus *and Comparison to the Highly similar Genomes of* Brucella melitensis *and* Brucella suis*."* Journal of Bacteriology 187:8 (2005): pp. 2715-2726.

Hoffmann M. R. *"Kinetics of the Oxidation of Sulfite by Hydrogen Peroxide in Acidic Solution."* The Journal of Physical Chemistry 79:20 (1975): pp. 2096-2098.

Jiménez de Bagués M. P., Terraza A., Gross A. and Dornand J. *« Different Responses of Macrophages to Smooth and Rough* Brucella *spp.: Relationship to Virulence."* Infection and Immunity 72:4 (2004): pp. 2429-2433.

Jones M. M. and Murphy T. F. *"Expression of the Oligopeptide Permease Operon of* Moraxella catarrhalis *Is Regulated by Temperature and Nutrient Availability."* Infection and Immunity 83:9 (2015): pp. 3497-3505.

Kasif S. and Steffen M. *"The evolution of gene annotation."* Nature Chemical Biology 6:1 (2010): pp. 4-5.

Kittelberger R., Hilbink F., Hansen M. F., Penrose M., de Lisle G. W., Letesson J.-J., Garin-Bastuji B., Searson J., Fossati C. A., Cloeckart A. and Schurig G. *"Serological crossreactivity between* Brucella abortus *and* Yersinia enterocolitica *0:9 I Immunoblot analysis of the antibody response to* Brucella *protein antigens in bovine brucellosis."* Animal Research 47 (1995): pp. 257-270.

Lampe D. J., Grant T. E. and Roberston H. M. *"Factors Affecting Transposition of the* Himar1 mariner *Transposon* in Vitro." Genetics 149:1 (1998): pp. 179-187.

Mailles A., Rautureau S., Le Horgne J. M., Poignet-Leroux B., d'Arnoux C., Dennetière G., Faure M., Lavigne J. P., Bru J. P. and Garin-Bastuji B. *"Re-emergence of brucellosis in cattle in France and risk for human health."* Eurosurveillance 17:30 (2012): pp. 9-11.

Mancilla M., Marin C. M., Blasco J. M., Zarraga A. M., Lopez-Goni I. and Moriyon I. *"Spontaneous Excision of the O-Polysaccharide* wbkA *Glycosyltransferase Gene Is a Cause of Dissociation of Smooth to Rough* Brucella *Colonies."* Journal of Bacteriology 194:8 (2012): pp. 1860-1867.

Mesner O., Riesenberg K., Biliar N., Borstein E., Bouhnik L., Peled N. and Yagupsky P. *"The Many Faces of Human-to-Human Transmission of Brucellosis: Congenital Infection and Outbreak of Nosocomial Disease Related to an Unrecognized Clinical Case."* Clinical Infectious Diseases 45:12 (2007): pp. 135-140.

Mitchell S. J. and Minnick M. F. *"Characterization of a Two-Gene Locus from* Bartonella bacilliformis *Associated with the Ability To Invade Human Erythrocytes."* Infection and Immunity 63:4 (1995): pp. 1552-1562.

Moreno E. and Moriyno I. *"The Genus Brucella"* The Prokaryotes 5 (2006): pp. 315-456.

Mutolo M. J., Jenny L. L.., Buszek A. R., Fenton T. W., and Foran D. R. *"Osteological and Molecular Identification of Brucellosis in Ancient Butrint, Albania."* American Journal of Physical Anthropology 147:2 (2011): pp. 254-63.

Myeni S., Child R., Ng T. W., Kupko III J. J., Wehrly T. D., Porcella S. F., Knodler L. A. and Celli J. "Brucella *Modulates Secretory Trafficking via Multiple Type IV Secretion Effector Proteins."* PLoS Pathogen 9:8 (2013).

Naroeni A. and Porte F. *"Role of Cholesterol and the Ganglioside GM in Entry and Short-Term Survival of* Brucella suis *in Murine Macrophages."* Infection and Immunity 70:3 (2002): pp. 1640-1644.

Pappas G., Papadimitriou P., Akritidis N., Christou L. and Tsianos E. V. *"The new global map of human brucellosis"* The Lancet infectious diseases 6:2 (2006): pp. 91-99.

Payne J. W. and Smith M. W. *"Peptide Transport by Micro-organisms."* Advances in Microbial Physiology 36 (1994).

Petersen T. N., Brunak S., von Heijne G. and Nielsen H. *"Signal P 4.0: discriminating signal peptides from transmembrane regions."* Nature Methods 8 (2011): pp. 785-786.

Pizarro-Cerda J., Méresse S., Parton R. G., Van Der Goot G., Sola-Landa A., Lopez-Goni I., Moreno E. and Gorvel J.-P. "Brucella abortus *transits through the Autophagic Pathway and Replicates in the Endoplasmic Reticulum of Nonprofessional Phagocytes."* Infection and Immunity 66:12 (1998): pp. 5711-5724.

Porte F., Liautard J.-P. and Köhler S. *"Early Acidification of Phagosomes Containing* Brucella suis *Is Essential for Intracellular Survival in Murine Macrophages."* Infection and Immunity 67:8 (1999): pp. 4041-4047.

Porte F., Naroeni A., Ouahrani-Bettache S. and Liautard J.-P. *"Role of the* Brucella suis *Lipopolysaccharide O Antigen in Phagosomal Genesis and in Inhibition of Phagosome-Lysosome Fusion in Murine Macrophages."* Infection and Immunity 71:3 (2003): pp. 1481-1490.

Pray, L. *"Transposons: The jumping genes."* Nature Education 1:1 (2008): pp. 204.

Roop II R. M., Gaines J. M., Anderson E. S., Caswell C. C. and Martin D. W. *"Survival of the fittest: how* Brucella *strains adapt to their intracellular niche in the host."* Medical Microbiology and Immunology 198 (2009): pp. 221-238.

Rudner D. Z., Le Deaux J. R., Ireton K. and Grossman A. D. *"The* spo0K *locus of* Bartonella subtilis *is Homologous to the Oligopeptide Permease Locus and Is Required for Sporulation and Competence."* Journal of Bacteriology 173:4 (1991): pp. 1388-1398.

Scholz H. C., Nöckler K., Göllner C., Bahn P., Vergnaud G., Tomaso H., Al Dahouk S., Kämpfer P., Cloeckaert A., Maquart M., Zygmunt M. S., Whatmore A. M., Pfeffer M., Huber B., Busse H-J., and Kumar De B. *"Brucella Inopinata Sp. Nov., Isolated from a Breast Implant Infection."* International Journal of Systematic and Evolutionary Microbiology 60:4 (2009): pp. 801-08.

Scholz H. C., Revilla-Fernandez S., Al Dahouk S., Hammerl J. A., Zygmunt M. S., Cloeckaert A., Koyglass M., Whatmore A. M., Blom J. Vergnaud G., Witte A., Aistleitner K. and Hofer E. *"Brucella Vulpis Sp. Nov., a Novel Brucella Species Isolated from Mandibular Lymph Nodes of Red Foxes (Vulpes Vulpes) in Austria."* International Journal of Systematic and Evolutionary Microbiology (2016).

Starr T., Child R., Wehrly T. D., Hansen B., Hwang S., Lopez-Otin C., Virgin H. W. and Celli J. *"Selective Subversion of Autophagy Complexes Facilitates Completion of the* Brucella *Intracellular Cycle."* Cell and Host Microbe 11:1 (2012): pp. 33-45.

Suarez-Esquivel M., Ruiz-Villalobos N., Castillo-Zeledon A., Jimenez-Rojas C., Roop II R. M., Comerci D. J., Barquero-Calvo E., Chacon-Diaz C., Caswell C. C., Baker K. S., Chaves-Olarte E., Thomson N. R., Moreno E., Letesson J.-J., De Bolle X. and Guzman-Verri C. "Brucella abortus *Strain 2308 Wisconsin Genome: Importance of the Definition of Reference Strains."* Frontiers in Microbiology 7 (2016).

van Opijnen T., Bodi K. L. and Camilli A. *"Tn-seq: high-throughput parallel sequencing for fitness and genetic interaction studies in microorganisms."* Nature Methods 6:10 (2009): pp. 767-772.

Vitry M-A., Hanot Mambres D., Deghelt M., Hack Katrin, Machelart A., Lhomme F., Vanderwinden J.-M., Vermeersch M., De Trez C., Pérez-Morga D., Letesson J.-J. and Muraille E. "Brucella melitensis *Invades Murine Erythrocytes during Infection."* Infection and Immunity 82:9 (2014): pp. 3927-3938.

Wattam A. R., Foster J. T., Mane S. P., Beckstrom-Sternberg S. M., Beckstrom-Sternberg J.M., Dickerman A. W., Keim P., Pearson T., Shukla M., Ward D. V., Williams K. P., Sobral B. W., Tsolis R. M., Whatmore A. M. and O'callaghan D. *"Comparative Phylogenomics and Evolution of the Brucellae Reveal a Path to Virulence."* Journal of Bacteriology 196:5 (2013): pp. 920-30.

Whatmore A. M., Dale E-J., Stubberfield E., Muchowski J., Koylass M., Dawson C., Gopaul K. K., Perrett L. L., Jones M. and Lawrie A. *"Isolation of* Brucella *from a White's tree frog (*Litoria caerulea). " JMM Case Reports (2015).

Williams K. P., Sobral B. W. and Dickerman A. W. *"A Robust Species Tree for the* Alphaproteobacteria. " Journal of Bacteriology 189:13 (2007): pp. 4578-4586.

Wu Q., Pei J. Turse C. and Ficht T. A. *"Mariner mutagenesis of* Brucella melitensis *reveals genes with previously uncharacterized roles in virulence and survival."* BMC Microbiology 6 (2006): pp. 102.

Yang X., Skyberg J. A., Cao L., Clapp B., Thornburg T. and Pascual D. W *"Progress in* Brucella *vaccine development."* Frontiers in Biology 100:2 (2013): pp. 130-134.

Yu N. Y., Wagner J. R., Laird M. R., Melli G., Rey S., Lo R., Doa P., Shainalp S. C., Ester M., Foster L. J. and Brinkman F. S. L. *"PSORTb 3.0: improved protein subcellular localization prediction with refined localization subcategories and predictive capabilities for all prokaryotes."* Bioinformatics 26:13 (2010): pp. 1608-1615.

Supplementary data

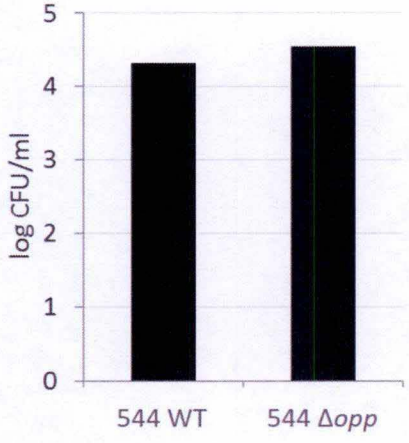

Figure S1 | Number of CFUs (logarithmic scale) for the 544 WT strain and its corresponding mutant after a 2 h infection in RAW 264.7 macrophages. Due to strong 2308 strains abnormalities, only the 544 results are shown here. Albeit not enough replicates were available to perform a statistical analyses, these results are interesting as they confirm the data obtained in the first 2 h PI CFU counting experiment.

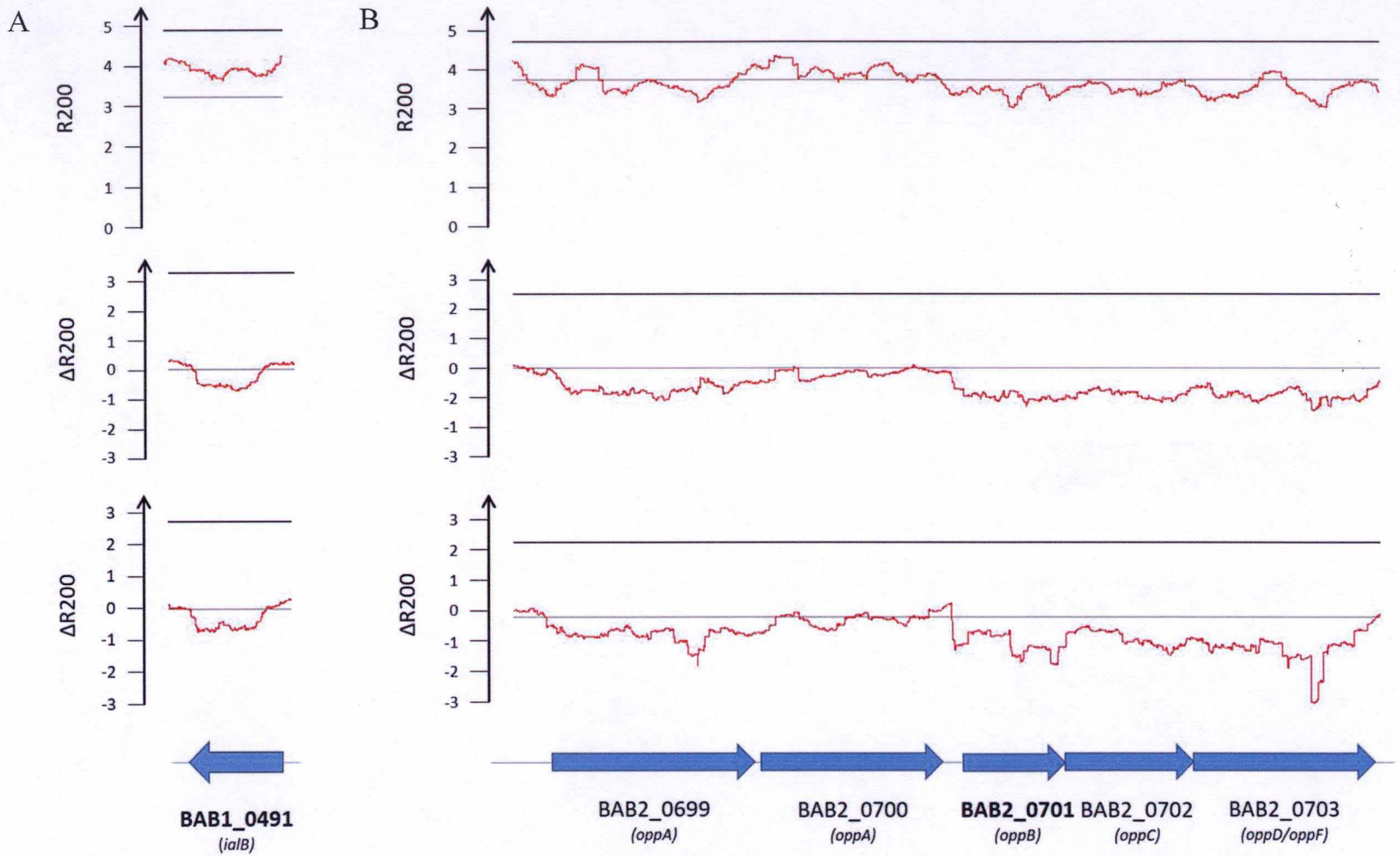

Figure S2 | Tn-seq profiles of *ialB* (A) and *oppB* (B) for the control, the 2h PI and the 24 h PI conditions. Each sub-figure follows the same pattern. The upper graph represents the control condition, the graph in between, the 2 h PI time point and the lower, the 24 h PI time point. The Y axis indicates the R200/ΔR200 values and the X axis, the genome map. The upper graph possess two straight lines; the light grey is the chromosomal mean transposon insertion number and the dark grey represents the maximum insertion number observed. Note that the two chromosome do not have the same transposon insertion values. On the two lower graphs, the dark grey is still representing the maxima but this time, the light grey line is centred at zero as this graph represent the delta of control and infection data (ΔR200). Therefore, when the red line (representing the delta between the control and the time point at a site) is below the light grey line that means that less mutants with an insertion at that site than the control value are observed, suggesting that a gene is important for a given condition.